Elsevier Editorial System(tm) for Journal of Volcanology and Geothermal Research
Manuscript Draft

Manuscript Number: VOLGEO5197

Title: Vapor Discharges On Nevado Del Ruiz During The Recent Activity: Clues On The Composition Of The Deep Hydrothermal System And Its Effects On Thermal Springs

Article Type: SI: VHSTaran

Keywords: Nevado del ruiz; geothermal system; equilibrium modelling; water chemistry; water isotopes

Corresponding Author: Dr. Cinzia Federico, Ph.D

Corresponding Author's Institution: Istituto Nazionale di Geofisica e Vulcanologia

First Author: Cinzia Federico, Ph.D

Order of Authors: Cinzia Federico, Ph.D; Salvatore Inguaggiato; Zoraida Chacón ; John M Londoño ; Claudia Alfaro ; Edwin A Gil

Abstract: The Nevado del ruiz volcano is considered one of the most active volcanoes in Colombia, which can potentially threaten approximately 600,000 inhabitants. The existence of a glacier and several streams channeling in some main rivers, flowing downslope, increase the risk for the population living on the flank of the volcano in case of unrest, because of the generation of lahars and mudflows. Indeed, during the November 1985 subplinian eruption, a lahar generated by the sudden melting of the glacier killed twenty thousand people in the town of Armero. Moreover, the involvement of the local hydrothermal system has produced in the past phreatic and phreatomagmatic activity, as occurred in 1989. Therefore, the physico-chemical conditions of the hydrothermal system as well as its contribution to the shallow thermal groundwater and freshwater in terms of enthalpy and chemicals require a close monitoring. The phase of unrest occurred since 2010 and culminated with an eruption in 2012, after several years of relative stability, still maintains a moderate alert, as required by the high seismicity and SO2 degassing.
In October 2013, a sampling campaign has been performed on thermal springs and streamwater, located at 2600-5000 m of elevation on the slope of Nevado del Ruiz, analyzed for water chemistry and stable isotopes. Some of these waters are typically steam-heated (low pH and high sulfate content) by the vapour probably separating from a zoned hydrothermal system. By applying a model of steam-heating, based on mass and enthalpy balances, we have estimated the mass rate of hydrothermal steam discharging in the different springs. The composition of the hottest thermal spring (Botero Londono) is probably representative of a marginal part of the hydrothermal system, having a temperature of 250°C and low salinity (Cl ~1500 mg/l), which suggest, along with the retrieved isotope composition, a chiefly meteoric origin.
The vapour discharged at the steam vent "Nereidas" (3600 m asl) is hypothesised to be separated from a high-temperature hyrothermal system. Based on its composition and on literature data on fluid inclusions, we have retrieved the P-T-X conditions of the deep hydrothermal system, as

well as its pH and fO2. The vapour feeding Nereidas would separate from a byphasic hydrothermal system characterised by the follow parameters: t= 315°C, P=15 MPa, NaCl= 15 %, CO2 = 5%, and similar proportion between liquid and vapour. Considering also the equilibria involving S-bearing gases and HCl, pH would approach the value of 1.5 while fO2 would correspond to the FeO-Fe2O3 buffer. Chlorine content is estimated at 6000 mg/l. Changes in the magmatic input into the hydrothermal system could modify its degree of vaporization and/or P-T-X conditions, thus inducing corresponding variations in vapour discharges and thermal waters. These findings, paralleled by contemporary measurements of water flow rates, could give significant clues on risk evaluation.

Suggested Reviewers: Bruce Christenson
GNS Science Wairakei Research Centre (NZ)
B.Christenson@gns.cri.nz

John Varekamp
Department of Earth & Environmental Sciences
jvarekamp@wesleyan.edu

Franco Tassi
Università di Firenze, Italy
franco.tassi@unifi.it

Dmitri Rouwet
Istituto Nazionale di Geofisica e Vulcanologia
dmitri.rouwet@ingv.it

Dear Editor,

Following my presentation at the session VHS Of AGU Fall meeting 2016, I submit my paper for the *"**VHSTaran** special issue of Journal of Volcanology and Geothermal Research"*

Please find attached the electronic source files related to the manuscript:

Vapor Discharges On Nevado Del Ruiz During The Recent Activity: Clues On The Composition Of The Deep Hydrothermal System And Its Effects On Thermal Springs

Federico C., Inguaggiato S., Chacón Z., Londoño J.M., Alfaro C.M., Gil E., Alzate D.

The Nevado del ruiz volcano is considered one of the most active volcanoes in Colombia, which can potentially threaten approximately 600,000 inhabitants. The existence of a glacier and several streams channeling in some main rivers, flowing downslope, increase the risk for the population living on the flank of the volcano in case of unrest, because of the generation of lahars and mudflows. In October 2013, a sampling campaign has been performed on thermal springs and streamwater, located at 2600-5000 m of elevation on the slope of Nevado del Ruiz, analyzed for water chemistry and stable isotopes. Some of these waters are typically steam-heated (low pH and high sulfate content) by the vapour probably separating from a zoned hydrothermal system. By applying a model of steam-heating, based on mass and enthalpy balances, we have estimated the mass rate of hydrothermal steam discharging in the different springs. The vapour discharged at the steam vent "Nereidas" (3600 m asl) is hypothesised to be separated from a high-temperature hyrothermal system. Based on its composition and on literature data on fluid inclusions, we have retrieved the P-T-X conditions of the deep hydrothermal system, as well as its pH and fO_2. Changes in the magmatic input into the hydrothermal system could modify its degree of vaporization and/or P-T-X conditions, thus inducing corresponding variations in vapour discharges and thermal waters. These findings, paralleled by contemporary measurements of water flow rates, could give significant clues on risk evaluation.

Suggested reviewers:

Bruce Christenson
GNS Science Wairakei Research Centre
114 Karetoto Road, Wairakei,
Private Bag 2000, Taupo,
New Zealand
Phone: +64-4-570 4640
Email: B.Christenson@gns.cri.nz.

Johan Warekamp
Johan (Joop) C. Varekamp
Department of Earth & Environmental Sciences
Exley Science Center, room 451, Wesleyan University
Telephone: 860 685 2248;
e-mail: jvarekamp@wesleyan.edu

Franco Tassi
Address: Università di Firenze
e-mail: franco.tassi@unifi.it

Dmitri Rouwet
INGV_Bologna
Italy
e-mail: dmitri.rouwet@ingv.it

I look forward to hearing about this manuscript

Best regards
Cinzia Federico

Vapor Discharges On Nevado Del Ruiz During The Recent Activity: Clues On The Composition Of The Deep Hydrothermal System And Its Effects On Thermal Springs

Federico C. [1*], Inguaggiato S. [1], Chacón Z.[2], Londoño J.M.[2], Alfaro C.M.[3], Gil E. [2], Alzate D.[2]

1 - Istituto Nazionale di Geofisica e Vulcanologia, sezione di Palermo, via U. La Malfa 153, 90146 Palermo

2- Servicio Geologico Colombiano, Observatorio Vulcanologico y Sismologico de Manizales, Avenida 12 de Octubre, 15 – 47, Manizales, Colombia

3- Servicio Geologico Colombiano, Diag. 53 N.° 34-53,Bogotá, Colombia

Abstract

The Nevado del ruiz volcano is considered one of the most active volcanoes in Colombia, which can potentially threaten approximately 600,000 inhabitants. The existence of a glacier and several streams channeling in some main rivers, flowing downslope, increase the risk for the population living on the flank of the volcano in case of unrest, because of the generation of lahars and mudflows. Indeed, during the November 1985 subplinian eruption, a lahar generated by the sudden melting of the glacier killed twenty thousand people in the town of Armero. Moreover, the involvement of the local hydrothermal system has produced in the past phreatic and phreatomagmatic activity, as occurred in 1989. Therefore, the physico-chemical conditions of the hydrothermal system as well as its contribution to the shallow thermal groundwater and freshwater in terms of enthalpy and chemicals require a close monitoring. The phase of unrest occurred since 2010 and culminated with an eruption in 2012, after several years of relative stability, still maintains a moderate alert, as required by the high seismicity and SO_2 degassing.

In October 2013, a sampling campaign has been performed on thermal springs and streamwater, located at 2600-5000 m of elevation on the slope of Nevado del Ruiz, analyzed for water chemistry and stable isotopes. Some of these waters are typically steam-heated (low pH and high sulfate content) by the vapour probably separating from a zoned hydrothermal system. By applying a model of steam-heating, based on mass and enthalpy balances, we have estimated the mass rate of hydrothermal steam discharging in the different springs. The composition of the hottest thermal spring (Botero Londono) is probably representative of a marginal part of the hydrothermal system, having a temperature of 250°C and low salinity (Cl ~1500 mg/l), which suggest, along with the retrieved isotope composition, a chiefly meteoric origin.

The vapour discharged at the steam vent "Nereidas" (3600 m asl) is hypothesised to be separated from a high-temperature hyrothermal system. Based on its composition and on literature data on fluid inclusions, we have retrieved the P-T-X conditions of the deep hydrothermal system, as well

as its pH and fO_2. The vapour feeding Nereidas would separate from a byphasic hydrothermal system characterised by the follow parameters:
t= 315°C, P=15 MPa, NaCl= 15 %, CO_2 = 5%, and similar proportion between liquid and vapour. Considering also the equilibria involving S-bearing gases and HCl, pH would approach the value of 1.5 while fO_2 would correspond to the FeO-Fe2O3 buffer. Chlorine content is estimated at 6000 mg/l. Changes in the magmatic input into the hydrothermal system could modify its degree of vaporization and/or P-T-X conditions, thus inducing corresponding variations in vapour discharges and thermal waters. These findings, paralleled by contemporary measurements of water flow rates, could give significant clues on risk evaluation.

Introduction

The Nevado del Ruiz volcano (NRV, 5321 m a.s.l.), is a stratovolcano located at the middle portion of the Central Cordillera of Colombia, and covers an area of approximately 200 km^2 (Figure 1). The NRV is located approximately 140 km NW of Bogota and 28 km SE of Manizales (4th 53' N, 75° 19' W). The NRV is considered one of the most active and dangerous volcanoes in Colombia, as in its area of influence live approximately 600,000 inhabitants in the towns of Villa María, Chinchiná, Murillo and Lebanon. From the top of NRV several streams originate, like Rio Lagunillas, Azufrado and Gualí, draining into the Magdalena River, and Rio Molinos, Nereidas and Alfómbrales streams, draining into the Cauca River. All these rivers represent a great threat to the population in case of a volcanic eruption, because the abrupt thawing of the glacial located in summit area of the volcano, and consequent channelling in the major rivers flowing downstream, can generate mudflows or avalanches, as occurred in the chatastrophic event of 1985.
The NRV is an open conduct volcano, with high SO_2 degassing plume (Krueger et al., 1990), characterized by the presence, on the summit area, of a wide fumarolic field with solfataric activity (Giggenbach et al. 1990; Barberi et al. 1990). Moreover, several very acidic thermal springs (Sturchio et. al, 1988, Sano et al., 1990; Alfaro et al., 2002; Inguaggiato et al., 2015) are located on the flanks of the edifice (Fig. 2) and make acidic also the rivers flowing downstream from the top of the volcano.
Several geochemical investigations were carried out during and after the catastrophic eruption occurred in 1985, that highlighted (even if a limited dataset is avalaible) the increase of both the SO_2/H_2S ratio in the vents at the solfataric summit area (Barberi et al. 1990) and the sulfate amount dissolved in the thermal springs. The eruption of 13 November, 1985 produced a huge SO_2 clouds emissions of 600 ktons (Krueger et al., 1990). In the weeks after the eruption, and particularly after 22 November, the SO_2 flux increased up to 10 kton/day (Williams et al., 1990).

Arango et al. (1970), according to the chemical composition of two groups of thermal waters (neutral chloride-bicarbonate and acidic chloride-sulfate), flowing at lower and at higher level (above 3000 masl) of volcano flanks, respectively, suggest the presence of an extensive geothermal system inside the NRV. Sturchio et al. (1988) confirm this hypothesis and, according to the chemistry of alkali-chloride waters, give an estimation of around 200°C for the deep hydrothermal reservoir. The same Authors also suggest that the high sulphate contents in thermal springs is due to the oxidation of H_2S coming directly from high-temperature magmatic gases. Giggenbach et al. (1990) propose that gases and waters from fumaroles and thermal springs on the flanks of the volcano are likely to be derived from a two-phase vapor-brine envelope surrounding the magmatic system.

In the last years, a strong increase of the SO_2 plume degassing was recorded by the UV-scanning DOAS monitoring network, operated by the Servicio Geologico Colombiano, peaking at 33 ktons/day in May-June 2012, paralleled by increased seismicity and several episodes of ash explosions (URL: http://www.ingeominas.gov.co/Manizales.aspx).

We report on the chemical and isotope composition of waters, collected in some thermal springs and rivers on the upper flanks of NRV in September-October 2013, and on gas chemistry of a low temperature fumarole on the Western flank of the volcano, collected in March 2016. We apply a steam-heating model (Federico et al., 2010) to account for the high sulfate and chlorine contents of steam-heated waters, and infer the original H_2S and HCl contents in the deep condensing vapour. As a result of the model, we estimate the mass contribution of this latter in every collected steam-heated waters. Moreover, according to the composition of a low-temperature fumarole on the Western flank of the volcano and some external contraints, we retrieve the physical-chemical conditions of the deep hydrothermal system and its pH and fO_2.

GEOLOGICAL FRAMEWORK

The study area of NRV is framed within the volcanic complex Cerro Bravo-Cerro Machin (Herd, 1982), where the tectonic environment is the result of the convergence of South American plate with Caribbean and Nazca plate and the micro-plates Coiba and Panama (Taboada et al., 2000; Bohorquez et al., 2005). This interaction between the plates is responsible for the different structural styles observed as well as for the geology of the investigated area. Recently, the volcanic Complex defined by Herd (1982) was catalogued as a Volcano-tectonic province, named Volcano-tectonic province of San Diego – Cerro Machín, which covers a large area with many other volcanoes and volcanic complexes (Martinez, 2014).

The NRV is located at the intersection of dominant fault systems oriented N-S, belonging to the Romeral Faults and NE-SW-trending Palestine Faults, which are consistent with the general directions of tectonic systems of Andean chain. This implies a strong tectonic control is this area, associated with the Andes orogenic cycle (Florez, 1992). Structures and kinematics in the region are closely related to the dominant tectonic features of the NVR, nominally longitudinal NE-SW and N-Sfaults (Palestina, Santa Rosa and San Jerónimo) and a transverse NW-SE to E-W system (Villamaría-Termales,Campoalegrito, San Ramón faults) (Mejia et al., 2012). Summarizing, locally Nevado del Ruiz is framed into four faulting systems: the Palestina fault, the NE-trending Nereidas-Olleta fault, the Villa María-Termales fault, the Nereidas and Río Claro faults (Martínez et al, 2014).

The geological units that make and integrate the core of the mountains are composed by metamorphic rocks of the Cajamarca complex and igneous rocks ranging from the Late Cretaceous (Stock of Manizales) to Early Eocene, where the location of intrusive bodies is represented by the Bosque batholith. The volcanic cover is made of pyroclastic deposits and lava flows mainly produced by Cerro Bravo, Santa Isabel and the Nevado del Ruiz volcanoes. Its eruptive history begins about 1.8 Ma ago and has been interpreted as divided into three phases: Ancestral Ruiz, Old Ruiz and Present Ruiz (Thouret et al., 1990). These phases consist of the building and subsequent destruction of the volcano edifice with the emplacement of lava flows, andesitic-dacitic lava domes and the deposition of volcano-sedimentary and volcano-clastic sequences. Nevado del Ruiz volcano now is considered a volcanic complex, named Nevado del Ruiz volcanic complex, due to the presence of several volcanic centres around it found recently (Martinez et al, 2014).

Historical Activity of NRV

The NRV in February 1845 registered a phreatic eruption (Internal Report Ingeominas, 1999), and then enters in a period of relative rest until 1984, when an intense increase of fumarolic and seismic activity was recorded close to the active crater.

After the increase of volcanic activity, a program of seismic monitoring started in July 1985 (Alvaro et al., 1990; Martinelli, 1990; Parra and Cepeda, 1990; Londoño, 2010a).

On 11 September 1985 a small phreatic eruption occurred and by November 13 of the same year a subplinian eruption started, with VEI = 3 (Calvache, 1986) which produced the melting of about 10% of the glacial mass (Naranjo et al, 1986), located on the summit of the NRV. The lahar

generated by the melting of the glacier buried the town of Armero (Tolima), killed twenty thousand peoples, and affected also the towns of Chinchiná (Caldas), Mariquita and Honda (Tolima).

On 1 September 1989, a second phreatomagmatic eruption occurred and, similarly to that of 1985, also generated a small lahar (Mendez and Valencia, 1995). The entire sequence of seismic activity was recorded in real time by the Volcanological and Seismological Observatory of Manizales (OVSM) of the Colombia Geological Survey (CGS), which had a telemetric network of short period seismic stations. After the eruptions of 1985 and 1989, frequent ash emissions were recorded, which continued for several years after (Londoño, 2010a, 2010b) accompanied by an active summit degassing (Stix et al., 2003). From 1992 to 2010, the volcano showed basically a stable volcanic activity with a reduced number of seismic events with progressively decreasing magnitude. Some increases of LP-type volcano earthquakes related with the dynamics of fluids occurred in July 1995 and June 2002. In January-July 2003, VT type volcano earthquakes related to rock fracturing were also recorded.

On 30 September 2010, the NRV showed an increase in the seismicity activity rates, particularly in terms of LP type earthquakes as well as hybrid earthquakes (HB), mainly located in the crater Arenas, at less of 2 km depth (García-Cano et al., 2011); in the same period a marked increase of SO2 plume emissions was also observed as well as important changes in volcanic deformation. From 1 October 2010 the alert level of activity of VNR was changed to Yellow Level (III of V levels). At the end of February 2012, a new ashfall was recorded, together with an increase in the seismic activity between March and April 2012, that marked the beginning of a new eruptive phase of NRV characterized by two eruptions, on May 29 and June 30. During 2013 and 2015 the seismic activity and the volatile degassing remained high, with activity alert level in Yellow.

Materials and Methods

A fumarole at boiling temperature (Nereidas) located on the west higher flank of the NRV, ten thermal springs and four acidic river flowing downstream from the upper flanks of Nevado have been collected and analyzed to investigate their chemical and isotopic composition (Fig. 2). At every site the outlet temperature, the electrical conductivity and the pH of the waters were measured using an ORION 250A+ conductimeter and thermometer and an ORION 250A+ pH-meter, respectively. The flow of each thermal spring and river have been estimated too. Water was sampled in polyethylene bottles in order to analyze its major components and its stable isotopes compositions. The samples for cations were filtered and acidified with ultrapure HNO_3. Alkalinity was determined in situ by titration with HCl 0.1 N, whereas major elements were analyzed in the laboratory using a Dionex-Thermo ICS 1100 ion chromatograph with an accuracy of ±2%. A

Dionex CS-12A column with CSRS 300 suppressor conductivity was used for the cations (Li, Na, K, Mg, Ca) and a Dionex AS14A-SC column with ASRS 300 suppressor conductivity was used for the anions (F, Cl, Br, NO_3, SO_4).

Dissolved gases were sampled and analyzed according to the method described by Capasso and Inguaggiato (1998) which is based on the headspace equilibrium partitioning of gaseous species between a liquid and a gas phase after the introduction of a host gas (Ar) into the sample.

Dissolved and free gases were analyzed by Perkin Elmer Clarus 500 gas chromatograph equipped with double detector (TCD, methaniser-FID configuration) using Ar as carrier gas and a Restek Shincarbon ST 3 m packed column.

The Nereidas fumarole was collected by pre-vacuum Giggenbach flask filled with sodium hydroxide 4 M connected via Dewar tube to a pipe inserted 50 cm into the fumarole emission (Giggenbach, 1975). The CO_2 content of the solution was analyzed by potentiometric titration, and for Stot, HCl, and HF according to the method described by Sortino et al. (1991). The head-space enriched gases, to determine He, H_2, O_2, N_2, CO, CH_4, were analyzed by gas chromatographic thecniques (Perkin Elmer Clarus 500) equipped with a Shincarbon ST 3 m packed column and double detector (hot-wire detector and flame ionization detector), with analytical errors lower than 3%. The H_2O content was determined by weighing the bottle before and after sampling, taking into account the absorbed amounts of CO_2 and acidic species, and finally the composition of the whole fumarolic gas was calculated accordingly (Badalamenti et al., 1991).

The Oxigen and Hydrogen isotopic composition of the water samples were determined using Analytical Precision AP 2003 and Thermo Finnigan Xp Plus IRMS interface to TC/EA respectively. The results are reported as δD and δ18O ‰ versus the V-SMOW standard, and the analytical precision was better than ±1% and ±0.1%, respectively.

Results

Water chemistry and stable isotopes

The chemical and isotopic composition of analysed waters are listed in Table 1. Collected samples have a total dissolved salt content (TDS) in the range 160 - 12800 mg/l, and temperature as high as 62.6°C.

According to major ion composition (Figure 2), most samples, characterized by temperatures in the range 6.8° - 62.6°C and acidic pH (between 1.2 and 3.6 units), fall in the field of steam-heated waters. These waters are typically SO_4-rich as an effect of condensation of S-bearing acidic gases. Among these, samples collected in Agua Calientes, Fuente Gualì and Hotel thermales hot springs are the hottest and most acidic ones, and among the most saline waters (2000 < TDS < 12800 mg/l).

Their saline content is reliably due to the hydrolisis of S-bearing gases, forming dissolved SO_4 ions, and marked leaching of the host rock through the titration of H^+ ions. This is evident in the pH-TDS graph of Figure 3, where the most saline samples are also characterized by the lowest pH values. The other steam-heated waters are samples collected in rivers and streams, flowing downstream from the upper flanks of Nevado. Their temperatures are generally low due to the rapid cooling of condensing vapour during flowing. The saline content depends on the amount of condensing vapour, it is generally below 2100 mg/l, with a maximum measured in Thermal La Gruta (4700 mg/l). Samples plotting in the field of perypheral waters are richer in CO_2, due to the selective and progressive removal of S-bearing gases from volcanic vapour during its travelling towards the surface. The samples richest in CO_2 (namely Rio Molinos, Agua Hedionda and Nereidas w., sampled in a stream flowing from Nereidas fumarole) have relatively higher pH, in the range 5.5-8.8, as an effect of the removal of acidic S-bearing gases during travelling. Only one sample (Botero Londono) has a Cl-rich composition, plotting in the field of chloride waters. It has a saline content of 1900 mg/l, pH 7.7, and a temperature of 79.5°C, the highest measured in that area. According to the Giggenbach's classification (1988), Botero Londono represents the most mature water, which has experienced a prolonged water-rock-interaction at depth.

Water stable isotopes indicate a clear meteoric origin for collected waters. Measured values for $\delta^{18}O$ range -15.4 to -11.1 ‰, and for δD from -114 to -91 ‰. In the scatter plot of Figure 4, where some literature data on Botero Londono and Agua Caliente are also reported (Sturchio et al., 1988), most samples are aligned along the GMWL ($\delta D = 8\ \delta^{18}O + 10$). Only two samples (Agua Caliente and Botero Londono thermal springs) show a slight oxygen-shift, and plot on the right of the GMWL. The composition of the vapour emitted from the Nereidas fumarole is markedly more negative than water samples ($\delta^{18}O$ = -21.2 ‰, δD = -135.4 ‰).

Gas chemistry

The chemical composition of fumarolic and dissolved gases is listed in Table 2.

The low temperature (t = 80°C) fumarole Nereidas, collected in March 2016, has steam content of 70 mol%, CO_2 = 25 mol%, Stot = 5%, CH_4 = 30000 μmol/mol, H_2 = 2200 μmol/mol, negligible CO and HCl < 70 μmol/mol. The prevailing sulfur species is H_2S, as measured by Giggenbach et al. (1990), accounting for by more than 80% ot total sulfur.

The analysis of dissolved gases indicates that atmospheric gases are the chief component in collected water samples, with variable contribution of CO_2, while CO, CH_4 and H_2 are only minor species (Figure 5). In particular, river waters (Rio Lagunillas, Rio Azufrado, Rio Gualì) are almost air saturated, due to their permanent exposure to the atmosphere. The lowest CO_2, CH_4 and CO

contents are measured in samples from Rio Gualì (2, 0.0001 and 0.00002 cc/l STP, respectively). The highest CO_2 and CH_4 contents are measured in Nereidas w. (360 and 0.05 cc/l STP, respectively), while the highest CO content is measured in the Agua Caliente thermal spring (0.005 cc/l STP). Hydrogen has been detected in only few samples, namely Hotel thermal springs (Hotel 1 and 2, with H_2 contents in the range 0.14-0.18 cc/l STP), Agua Caliente, Botero Londono and FT Gualì.

Discussion

The Nevado del ruiz hydrothermal system

Geothermometric estimation : water-rock equilibria

Chloride-rich, neutral pH and hot waters (t= 80°C) collected in Botero Londono likely represent the saline liquid phase of the local hydrothermal system, partially diluted by meteoric water. The characteristics of the Botero Londono thermal water comply those expected for the liquid phase in hydrothermal systems.

In a biphase hydrothermal system, after steam separation, the liquid phase is enriched in chemicals and isotopes having stronger affinity for the liquid phase with respect to the vapour. In particular, at hydrothermal P-T conditions, while H_2S and CO_2 partition in the vapour phase, Cl is preferentially enriched in the liquid phase. Analogously, water heavier isotopes preferentially partition in the liquid phase below 220 °C, according to enrichment factors. The pH of the residual liquid, after vapour separation, is near-neutral because of both the loss of acidic gas species in the vapour phase and rock titration.

As suggested by Giggenbach et al. (1990), the water from Botero Londono wells, among the collected hot samples, appears to be the relatively most mature and, therefore, the most suitable for thermometric estimations. As the water chemical composition does not reflect full equilibrium with the host rock, as deduced from the triangular diagram of Figure 6, we follow the approach proposed by Reed and Spycher (1984). Following this method, we compute the saturation index with respect to a series of possible alteration minerals at various temperatures through PHREEQC code (Parkurst and Appelo, 1999), operating with the LLNL (Lawrence Livermore National Laboratory) database. To ensure the consistency of thermodynamic data for secondary minerals, namely logK and ΔH for dissolution reactions, we select from the database only those minerals derived from the SUPCRT92 database (Johnston et al., 1992). The results of the simulations are shown in Figure 7. According to the proposed approach, the temperature range where the saturation index is nearly 0 for most minerals should indicate the equilibrium condition and would give the most likely estimate

of reservoir conditions. As observed, the saturation index with respect to many Al-silicates (namely Illite, Muscovite, Albite, Anorthite, K-Feldspar, Wairakite, Laumontite, Quartz) is close to 0±0.25 in the range 180-225°C. The water appears in equilirium with Calcite and amorphous Silica at almost outlet temperature, and at the saturation with respect to Gibbsite, Kaolinite and Chalcedony in the range 125-150°C. These findings would suggest that thermal waters circulate in a zoned hydrothermal system (Giggenbach et al., 1990), where thermal fluids equilibrate at lower temperature with some secondary minerals, characterised by faster kinetics of precipitation. The zoning of the hydrothermal system probably results from the infiltration at depth of shallow and cold meteoric water and snow. As theorized by Reed and Spycher (1984), the possible dilution upon ascent is envisageable from the scattering of saturation indexes observed in Figure 7a. This scattering can derive, otherwise, from the lack of overall equilibrium with the secondary minerals.

On these grounds, we propose to retrieve the composition of the deep hydrothermal fluid, assuming that the composition of Botero Londono water results from the mixing between shallow cold water (here represented by the sample collected in the nearby Rio Molinos) and a deeper end member. The maximum fraction of the cold end member, allowed by the mass balance, would be 0.35. After then, for the obtained solution, we re-computed the saturation indexes with respect to a set of secondary minerals, assuming that, given its fast kinetics, the water is always at equilibrium with calcite, and the results are shown in Figure 7b. As observed, the obtained solution, i.e. the undiluted thermal water, appears almost at equibrium with secondary Al-silicates, namely Illite, Muscovite, Albite, Anorthite, K-Feldspar, Wairakite, Laumontite, Quartz, in a narrower and higher temperature range, between 225 and 250°C. Gibbsite, Kaolinite and Chalcedony, for their faster kinetics, represent an equilibrium at temperature 175-200°C, while the saturation index with respect to amorphous silica is once again indicative of outlet temperature. Hydrothermal secondary minerals collected in proximity of thermal springs reveal a prevalently argillitic alteration, with an assemblage of Kaolinite, clay minerals (Illite, Illite-Smectite), Feldspar, Calcite, Gypsum, Chalcedony (Forero et al., 2011). The maximum estimated temperature, according to the available data, for the hydrothermal fluid is therefore 250°C, while the estimated lower temperature reliably results from both the dilution with shallow water and cooling upon travelling towards the surface. The water composition, retrieved by considering a dilution fraction of 0.38, is listed in Table 3. The undiluted solution would contain 2200 mg/kg of Cl, 1360 mg/kg of Na, 308 mg/l of SiO_2.

According to the hypothesised dilution factor of 0.38, the entalpy balance (computed from the steam tables from Wagner and Overhof, 2006) would provide, for the mixed solution, a temperature of 166°C:

$$H_{dil} = y \cdot H_{15} + (1-y) \cdot H_{250} \qquad [1]$$

where H_{dil}, H_{15} and H_{250} represent the enthalpies of the diluted water, and the 15° and 250°C end members, while y is the molar fraction of the 15°C end member. This temperature is compatible with that estimated for Botero Londono according to the the saturation with respect to Gibbsite, Chalcedony and Kaolinite, representing a colder equilibrium zone within the hydrological system. The equilibrium temperature retrieved from the ^{18}O-isotope equilibrium sulfate-water provided an estimated temperature of 187°C (Giggenbach et al., 1990), compatible with the temperature computed for the colder equilibrium. The diluted solution probably undergoes further cooling upon ascent, via steam separation or conductive cooling, until the outlet temperature, measured at Botero Londono.

Based on the mass balance computation, it is also possible to retrieve the water isotope composition of the 250°C end-member:

$$\delta_{dil} = y \cdot \delta_{15} + (1-y) \cdot \delta_{250} \qquad [2]$$

where δ_{dil}, δ_{15} and δ_{250} are the isotope compositions of the diluted water (Botero Londono, Table 1), and the 15° (Rio Molinos, Table 1) and 250°C end members. The obtained isotope composition of the deep water is δD = -90.8 ‰, $\delta^{18}O$= -9.9 ‰. Represented on the δD-$\delta^{18}O$ plot of Figure 4, it appears still in a range compatible with an origin typically meteoric, although shifted for ^{18}O.

Geothermometric estimation : CH_4/CO_2 and CO/CO_2 log ratios

Based on the CO_2, CH_4, H_2 and H_2O of Nereidas fumarole (Table 1), a deep equilibrium temperature has been estimated, according to the relationship

$$CH_4 + O_2 = CO_2 + H_2O \qquad [3]$$

and assuming fH_2O fixed by the liquid-vapour equilibrium

$$fH_2O = 4.9\text{-}1820/T \qquad [4]$$

valid for brines (Giggenbach, 1980). Concerning the fO_2, the value of Log(H_2/H_2O) molar ratio measured in the Nereidas fumarolic sample is -2.5 (Log(H_2/H_2O) = -2.7; Giggenbach et al., 1990), close to the value -2.8, attributed to the FeO-Fe_2O_3 buffer (Giggenbach, 1980). The obtained temperature for the deep equilibrium is 290°C, slightly lower than the estimate of 315°C, based on previous data (Giggenbach et al., 1990).

The chemical composition of dissolved gases could allow an estimation of deep temperatures, bearing in mind some possible bias, related to water-gas reactions.

By the inspection of Table 2, we can notice significant amount of CO, comparable to CH_4, in some high temperature samples, namely Agua calientes, Hotel thermales 1 and 2, Botero Londono, Ft Gualì. In the triangular graph of Figure 8 (CO_2, CO, CH_4), most samples, with the exception of Nereidas, Agua Blanca and Agua Hedionda, are significantly enriched in CO with respect to

samples collected in the crater fumaroles (Barberi et al., 1990; Giggenbach et al., 1990), despite their likely equilibration in a shallower and reduced environment, compared to magmatic gases.

The production of CO occurs according to the so-called water-shift reaction (WSR) in the vapour phase

$CO_2 + H_2 = CO + H_2O$ [5]

through the consumption of CO_2 and H_2 in reducing environment.

The WSR equation can be rewritten as

$CO_2 = 0.5O_2 + CO$ [6]

by combining equation 5 and the reaction of water dissociation

$H_2O = 0.5O_2 + H_2$. [7]

The WSR is rapid at temperature higher than 300°C, but its kinetics becomes sluggish at lower temperature, as observed by Seewald et al. (2006). This ensures the preservation of high temperature CO/CO_2 equilibrium upon cooling. Nevertheless, the geothermometric estimations based on the WSR reaction, with fO_2 fixed by the $FeO\text{-}Fe_2O_3$ buffer, provide irrealistic temperatures, in some cases higher than 500°C. The exceptionally high CO relative abundances, measured in steam-heated waters, could derive, instead, from redox equilibria involving sulfur-bearing species in aqueous solutions, as proposed by Shock et al. (2010)

$4HCO_3^- + 2H^+ + H_2S_{aq} = 4CO + 4H_2O + SO_4^{--}$ [8]

According to this reaction, H_2S_{aq}, in acidic environment, as that characterizing steam-heated waters, is oxidized to form SO_4^{--} ions, while HCO_3^- is reduced to gaseous CO. Actually, preliminary speciation calculation of steam-heated samples (not shown) indicates SO_4^{--} as the prevailing S species, while H_2S should exist only at very low concentrations, despite the fact that the pristine hydrothermal gas should contain H_2S_g as the main S-bearing gas. The production of CO in such conditions would alter the temperature estimate, based on the WSR reaction. Indeed, the CO excess has been measured in steam-heated water samples, where reaction 8 likely occurs.

With this in mind, the thermometric calculations have been based essentially on CH_4/CO_2 ratios, deriving from equation 3, by considering CO/CO_2 only for CO_2-rich samples, namely Nereidas, Agua Blanca and Agua Hedionda. The $LogCO/CO_2$ ratios measured in collected samples are plotted together with $LogCH_4/CO_2$ ratios in the diagram of Figure 9. In the graph, the curve relative to the buffer $FeO\text{-}F_2O_3$ is plotted, by fixing fH_2O according to equation 4, along with the curve representing equilibrium in a saturated liquid phase (Chiodini and Marini, 1998). As observed, sampled waters have an almost homogeneous $LogCH_4/CO_2$ ratios, while they differ significantly for the $LogCO/CO_2$. In particular, sulphate-rich steam-heated waters plot on the right of the $FeO\text{-}Fe_2O_3$ curve, which represents equilibrium in a single saturated vapour phase, thus falling in the field of

super-heated vapour. This finding, unlikely for low temperature dissolved gases, is reliably related to the above described redox reaction in S-rich waters. Samples Nereidas, Agua Blanca and Agua Hedionda, typically perypheral waters, plot in the liquid field, at temperature close to 300°C, thus representing a vapour equilibrated in a liquid phase, which has experienced vapour loss in some cases (Agua Hedionda and Agua Blanca).

The steam-heating process

Hot and sulfate-rich waters, namely Agua Caliente and Hotel termales springs (samples Hotel 1 and 2), are reliably steam-heated waters, according to the classification proposed by Giggenbach (1988). The origin of the steam could be the vapour separating from the hydrothermal system or the magmatic vapour, presently emitted from the crater vents and condensing along fractures during the ascent within the volcanic conduits.

The amount of SO_4^{2-} or Cl^- in the steam-heated waters would be controlled by the relative mass fluxes of local cold groundwater and deep volcanic vapour, other than the concentration of the acidic gases in the volcanic vapour. The relative concentrations of Cl^-, SO_4^{2-}, and C_{tot} as well as water stable isotopes can ultimately provide clues about changes in the input of deep vapor into the shallow water bodies relative to that from the shallow groundwater. To model the steam-heating process, we apply the approach proposed by Federico et al. (2010), based on the following heat and mass-balance equations:

$$\sigma H_{l,c} + \phi H_{v,d} - \varpi H_{v,sh} = (\sigma + \phi - \varpi) H_{l,sh} \quad [9]$$

$$\sigma m_{l,c} + \phi m_{v,d} - \varpi m_{v,sh} = (\sigma + \phi - \varpi) m_{l,sh} \quad [10]$$

$$\sigma \delta_{l,c} + \phi \delta_{v,d} - \varpi \delta_{v,sh} = (\sigma + \phi - \varpi) \delta_{l,sh} \quad [11]$$

where σ, ϕ, and ω are the mass fluxes of the cold shallow water, the deep vapour, and the vapour separated from steam-heated water, respectively; subscripts *l* and *v* refer to the liquid and vapor phases, respectively; subscripts *sh*, *c*, and *d* indicate the steam-heated, cold, and deep endmembers, respectively; *H* is the enthalpy (computed from Wagner and Overhof, 2006); *m* is the molal concentration of chemicals; δ stands for the $\delta^{18}O$ or δD isotope composition. According to the model, the pristine composition of sampled thermal waters is modified by the process of steam heating and reboiling or, in other words, by both the input of chemicals and the enthalpy from the ascending vapor and the consequent steam separation. In the model, as the mass fluxes of the cold aquifer and the deep steam are not constrained, we assume that different ϕ/σ ratios are possible. The other fixed parameters are the chemical and isotopic composition of cold water and deep steam, while the flux and composition of the separating steam derive from the solution of equations 9-11.

The boundary conditions for the deep vapour, the cold meteoric recharge, and the steam-heated waters are listed in Table 4. The S_{tot} and HCl contents in the deep vapour are fixed by assuming that it has the same composition as the Nereidas fumarole, namely S_{tot} = 1%. For the HCl content in the deep vapour, we use a trial and error approach, due to the very low HCl content measured in the Nereidas fumarole, which provide an estimation of HCl content of 0.4% in the deep vapour phase. Given the low temperature of this fumarole (80°C), we can hypothesize phenomena of partial condensation and HCl removal during ascent, due to the strong its affinity for the liquid phase at low temperature (Liotta et al., 2010). The partial condensation of the ascending vapour would imply a two-step steam-heating model, where the mass flux, enthalpy and composition of the vapour condensing in the second (shallower) step (namely ϕ, $H_{v,d}$ $m_{v,d}$ and $\delta_{v,d}$) are those of the vapour separating in the previous step (ϖ, $H_{v,sh}, m_{v,sh}, \delta_{v,sh}$). The computations are performed whilst assuming that the condensation occur always at temperature of 100°C, in a cold aquifer at the initial temperature of 10°C. The isotopic composition and solute contents of the cold-water recharge are therefore fixed accordingly. In the first step of condensation, the mass flux of cold water is 1.5-5 % of the mass flux of the deep vapour. The presence of this very low amount of liquid water is, however, able to drastically reduce both S_{tot} and HCl from the vapour phase; the resulting composition of the separating vapour would be S_{tot} = 0.03-0.4 % and HCl = 0.01-0.1 %. Details of the modelization are described in Appendix 1. The results of the steam-heating model are plotted as curves linking the points representative of different ϕ/σ ratios in Figures 4 and 10, along with the composition of both the sampled thermal waters and the Nereidas fumarole. The dots along the curves represent different ratios of deep steam to cold water (i.e., ϕ/σ**)**. According to the model, the increasing amount of condensing vapour (i.e. larger deep-steam/cold-water mass ratios) implies higher SO_4 and Cl contents, as well as heavier isotope composition. Literature data on thermal waters are taken from Sturchio et al. (1988). Model results allow to retrieve for each sample the deep-steam/cold-water mass ratios (from ϕ/σ), and to identify the sites most affected by the input of condensing deep vapour. For the Agua Calientes thermal springs, the ratio ϕ/σ is 0.48: t his figure, coupled with the value of the water yield, gives an estimate of the deep vapour flux of 1 l/s (Table 1). Thermal waters of Hotel Thermales, fitted by a ϕ/σ of 0.46, are entered by a comparatively higher vapour flux, estimated in 7.7 l/s (Table 1). In the same area, Thermal La Gruta and Quebrada La Gruta, tough being ipothermal waters with relatively lower SO_4 and Cl contents, are entered by a significant mass of vapour, 2.4 and 20 l/s respectively (Table 1).

Concerning stable isotopes, collected samples plot very close to the meteoric water line, excepting steam-heated waters, appearing slightly shifted for $\delta^{18}O$ (Figure 4). The slight enrichment in heavy

isotopes is thought as due to the condensation of a deep vapour, which isotope composition can only be hypothesized. The isotope composition of a undiluted deep fluid at 250°C has been estimated in section *"Geothermometric estimation : water-rock equilibria",* starting from the composition of Botero Londono. We recall here the composition of this liquid, being δD = -90.8 ‰, $\delta^{18}O$= -9.9 ‰. The composition of the vapour in equilibrium with this liquid, at temperature of 250-315°C (as resulting from geothermometers), would be δD = -88.4/-85.6 ‰, $\delta^{18}O$= -11.5/-12 ‰. This composition is in agreement with that of a steam sample collected in a crater fumarole on July 1985 (δD = -89 ‰, $\delta^{18}O$= -12.9 ‰; Bulletin Global Volcanism Program). The isotope composition of the condensing steam is therefore fixed at δD = -87 ‰, $\delta^{18}O$= -11.75 ‰. In Figure 4, the curve representing the steam-heating process is plotted, hypothesizing the condensation at temperature of 100°C (conductive cooling down to the average outlet temperature of steam-heated waters is envisaged). Even in the case of stable isotopes, a two-steps steam heating process is considered, although the first partial condensation does not modify significantly the isotope composition of the vapour. The reliability of the steam-heating modelling is confirmed by the relationship $\delta^{18}O$ - Cl (Figure 10b).

The deep hydrothermal aquifer

According to what discussed so far, the Nereidas fumarole is fed by the vapour separating from a boiling hydrothermal aquifer, condensing at shallow depth in a steam-heated aquifer, locally discharging at the thermal springs of Hotel thermales, Quebrada La Gruta, Thermal La Gruta and Agua Calientes.

In this chapter, we try to retrieve the composition, pH and fO_2 of the deep hydrothermal system, according to the composition of the Nereidas fumarole. Assuming a boiling hydrothermal system at the maximum temperature estimated in section *geothermometric estimations* (315°C), the vapour emitted by the Nereidas fumarole must have undergone cooling upon ascent. We thus compute PTX conditions of the deep hydrothermal system according to the composition of Nereidas fumarole, by taking into account eventual processes able to modify the composition of the hydrothermal vapour upon ascent and cooling down to the sampling conditions (80-100°C).

Data on the vapour composition measured in Nereidas in 2016, listed in Table 2, indicate a vapour-dominated vapour, with H_2O contents of 70 mol% and CO_2 = 25 mol%. In the steam condensate collected on October 2013, 2.7 μmol/mol of NaCl have been measured. By hypothesing a vapour separation from a biphase system, prevalently fed by meteoric water and having a certain salinity, we consider the system H_2O-CO_2-NaCl at temperature of 315°C at depth, as obtained by

geothermometric estimations. The NaCl content in the deep fluid is retrieved from recent analyses of fluid inclusions in carbonates, considered as representative of the hydrothermal fluid (Uruena-Suarez et al., 2012). These fluid inclusions are bifasic, with the liquid phase slightly prevailing over the vapour one, and have a NaCl content of 15% on average. As further constraint, we fix fCO_2, as computed by assuming equilibrium with a hydrothermal paragenesis made of calcite, a Ca-Al-silicate, K-feldspar, K-mica and Chalcedony (Chiodini and Marini, 1998), according to the equation:

$\log fCO_2 = 0.0168\ t°C - 3.78.$ [12]

At 315°C, equation 12 provides a $fCO_2 = 33$ atm.

Alternatively, fCO_2 can be computed from the vapour composition and the externally fixed fH_2O according to the reaction

$CH_4 + 2H_2O = 4H_2 + CO_2$ $\log K_{CH4}$ [13]

modified as follows

$\log fCO_2 = \log K_{CH4} - 3\log(\chi H_2/\chi H_2O) - \log(\chi H_2/\chi CH_4) - \log fH_2O.$ [14]

The computed fCO_2 is 36 atm, comparable to the value obtained from equation 12.

We therefore apply the equation of state proposed by Anderko and Pitzer (1993), by means of LONER AP - software package Fluids (Bakker, 2003; http://fluids.unileoben.ac.at/Computer.html), by selecting a bulk composition of the hydrothermal system, in terms of H_2O, CO_2 and NaCl, able to satisfy specific constraints, to obtain the composition of the two phases and the pressure of the hydrothermal sytem. The constraints in such a system are:

temperature = 315°C

$NaCl_{bulk}$ = 10-15 % wt

fCO_2 = 32-36 atm.

Furthermore, as found in fluid inclusions, the hydrothermal system is hypothesised as biphasic, with slight prevalence of the liquid phase: the steam fraction is fixed at 0.45 - 0.46.

The results of the computations, obtained for a narrow range of plausible values, compatible with the fixed constraints, are graphically shown in Figure 11. At temperature of 315°C and NaCl concentration of 10-15%, the equilibrium pressure woud be 15 MPa. In these conditions, and satisfying the other constraints on fCO_2 and steam fraction, the vapour phase should be contains 0.22-0.23 mol/mol of CO_2, while the CO_2 content in the bulk fluid would be 2.3% mol. This deep vapour has a CO_2 content compatible with the values measured in Nereidas fumarole (χCO_2 = 25 mol%).

Given the equilibrium composition of both the liquid and the gaseous phases in the system H_2O-CO_2-NaCl (Table 5) and the molar fraction of the other gaseous species, as averaged from the

composition of the Nereidas fumarole (this study and Giggenbach et al., 1990), we try to assess pH, fO_2 and the concentration of some major ions in the deep hydrothermal system, at temperature of 315°C and pressure of 150 bar. Given the very low HCl content of Nereidas fumarole, probably related to fractional condensation during ascent (Liotta et al., 2010), we need to recompute the HCl concentration at equilibrium PTX conditions. The modelling requires some equilibria to be satisfied, as described below. Given the salinity recomputed for the deep hydrothermal fluid, the activity coefficients have been calculated according to the Debye Hückel expression. The fugacity coefficients for $CH_{4(g)}$ and H_2 are from Spycher and Reed (1988). As for these gases, the fugacity coefficient is close to 1, we make the same assumption also for S-species and HCl. The fugacity coefficient of steam, NaCl(g) and $CO_{2(g)}$ are derived from LONER AP.

We consider the equilibria involving chlorine species, namely $HCl_{(g)}$, Cl^-, $NaCl_{aq}$ and HCl_{aq}, sulfur species ($H_2S_{(g)}$, $SO_{2(g)}$, SO_4^{--}, SO_3^{--}, HSO_3^-, HSO_4^-, HS^-, $H_2S_{(aq)}$, S^{--}), carbon species ($CO_{2(g)}$, $CH_{4(g)}$, $CO_{2(aq)}$, $CH_{4(aq)}$, HCO_3^-, CO_3^{--}), $O_{2(g)}$, water dissociation ($H_2O = H^+ + OH^-$) and elettroneutrality. The final equilibrium composition of the liquid phase, as well as the gaseous phase, is computed by using a code for the minimization of Gibbs free energy (HSC Chemistry 6.1). The final equilibrium composition is listed in Table 6a.

In this system, the input data are temperature and pressure, the moles of CO_2, NaCl and H_2O in both the liquid and the gaseous phases, the vapour fraction as derived from EOS computations with LONER software, and the molar fraction of CH_4, H_2, HCl, CH_4, SO_2 and H_2S in the gaseous phase. The concentration of dissolved species, fO_2, and pH are unknowns.

The computed LogfO_2 at equilibrium is -32.1 at 315°C, corresponding to the value expected from the buffer FeO-Fe2O3, typical of hydrothermal systems. In these conditions, $SO_{2(g)}$ is not stable, as results from Table 6a. The coexistence of CH_4 and SO_2 in the vapour collected in Nereidas would suggest that the full equilibrium is not accomplished in the hydrothermal system, being continuously fluxed by oxidized SO_2-rich magmatic gases. The computed pH of the hydrothermal system is 3.2. The presence of NaCl in the system and acidic conditions favour the partition of HCl in the vapour phase, at concentration significantly higher than that measured in Nereidas fumarole, and provided as input for HSC calculations (χ_{HCl} = 0.00007, Table 2). The equilibrium contents of both HCl and H_2S are very close to the those fixed as boundary condition for the *steam-heating model*, and are plotted for reference in Figures 10a,b. In the acidic conditions estimated for the deep aquifer, undissociated dissolved species prevail, namely $CO_{2(aq)}$, $HCl_{(aq)}$, and $H_2S_{(aq)}$.

The equilibrium Cl^- content in the hydrothermal liquid is 10300 mg/kg. This value is higher than that recomputed from the sample collected in Botero Londono, according to the thermometric considerations and mass balance calculations described above, and quantified in 2200 mg/kg. This

finding would imply that the thermal water discharging at Botero Londono comes from a marginal part of the hydrothermal system, which undergoes a partial dilution at depth while being still heated at 250°C, as discussed in *section water-rock equilibria*, before ascent and further dilution close to the surface.

By hypothesizing gas-water-rock equilibrium in the hydrothermal system, we compute the minimization of Gibbs free energy by including a solid phase, made of minerals resulting at equilibrium at 250°C with the parent fluid of Botero Londono (*Geothermometric estimations*). In the simulation, we hypothesize 1 mole of each mineral, giving 2 kg of solid, in equilibrium with 1 kg of water. The obtained water/rock ratio is compatible with those expected in geothermal systems (Larson and Taylor, 1986; White et al., 1992). Although the real hydrothermal paragenesis is unknown, these minerals, namely K-, Na- and Ca-Feldspars, Laumontite, Wairakite, Illite, Kaolinite, Quartz and Calcite, are commonly observed in hydrothermal systems (Giggenbach, 1988). The results of computations are listed in Table 6b. As observed, the most significant difference with respect to the gas-water system is the equilibrium pH (pH = 4.9), higher than the former equilibrium, but still acidic. The solid assemblage computed at equilibrium includes Quartz, Calcite, Wairakite, Illite.

Modification of the deep vapour composition: possible processes

The vapour emitted from low-temperature fumaroles in NdR system can change over time due to either modification in the deep hydrothermal system and in the vapour in equilibrium or to secondary processes related to ascent and cooling. Let's first consider eventual fractionation processes affecting the vapour upon ascent, according to what already discussed in previous sections about the steam-heating process. The vapour emitted from Nereidas has undergone a cooling of 200°C at least, and its composition could have been modified either by further steam separation, according to an isohentalpic process, or by condensation, after cooling in the shallow environment, where cold water circulates. According to the first process, further steam separation would decrease the concentration of CO_2 with respect to water vapour, according to the following henthalpy and mass balance equations:

$$H_{bulk,315} = yH_{s,315} + (1-y)H_{l,315} \qquad [15]$$

where H denotes enthalphy, the subscripts *bulk*, *s*, and *l* indicate the biphase system, the vapour and the liquid phases, respectively, at 315°C, y is the fraction of vapour in the biphasic system. The isoenthalpic cooling implies:

$$H_{bulk,315} = sH_{s,100} + (1-s)H_{l,100} \qquad [16]$$

where *s* is the steam fraction separated after single step steam separation from 315 to 100°C. In these conditions, the steam fraction *s* at 100°C will be higher than the initial steam fraction *y* at 315°C. Similarly, the mass balance for CO_2 would imply

$$\left(\frac{\chi_{CO_2}}{\chi_{H_2O}}\right)_{bulk,315} = y\left(\frac{\chi_{CO_2}}{\chi_{H_2O}}\right)_{s,315} + (1-y)\left(\frac{\chi_{CO_2}}{\chi_{H_2O}}\right)_{l,315} \quad \text{and}$$

$$\left(\frac{\chi_{CO_2}}{\chi_{H_2O}}\right)_{bulk,315} = s\left(\frac{\chi_{CO_2}}{\chi_{H_2O}}\right)_{s,100} + (1-s)\left(\frac{\chi_{CO_2}}{\chi_{H_2O}}\right)_{l,100}, \text{ which can be written as}$$

$$\left(\frac{\chi_{CO_2}}{\chi_{H_2O}}\right)_{bulk,315} = s\left(\frac{\chi_{CO_2}}{\chi_{H_2O}}\right)_{s,100} + (1-s)\frac{1}{B_{CO_2,100}}\left(\frac{\chi_{CO_2}}{\chi_{H_2O}}\right)_{s,100} \qquad [17]$$

where $\frac{\chi_{CO_2}}{\chi_{H_2O}}$ is the molar ratio CO_2/H_2O and $B_{CO_2,100}$ is the vapor/liquid partition coefficient of CO_2 at 100°C. In equation 17, the last term can be neglected due to low value of $\frac{1}{B_{CO_2,100}}$. With a steam fraction *s* as computed from the enthalpy balance (eq. 16), the $\frac{\chi_{CO_2}}{\chi_{H_2O}}$ would be decreased in the 100°C vapour. In case of HCl, having very low B values, particularly at lower temperature, in the order of magnitude of $10^{-3}/10^{-4}$, the cooling would imply the drastic drop of HCl contents of the original vapour and negligible HCl contents in the vapour phase at the outlet temperature of fumaroles, as observed in Nereidas fumarole.

As an alternative cooling process, we consider adiabatic condensation, which should enrich CO_2 in the vapour phase as long as water is removed from the vapour. The mass balance equation for steam condensation is

$$\left(\frac{\chi_{CO_2}}{\chi_{H_2O}}\right)_{bulk,315} = (1-c)\left(\frac{\chi_{CO_2}}{\chi_{H_2O}}\right)_{s,100} + c\frac{1}{B_{CO_2,100}}\left(\frac{\chi_{CO_2}}{\chi_{H_2O}}\right)_{s,100} \qquad [18]$$

where *c* is the fraction of condensed liquid water. Even in this case, the condensation of water would drive also the condensation of the most soluble species, namely HCl, drastically reducing their content in the residual vapour.

Once analyzed the possible secondary processes, able to modify the pristine composition of vapour, we now consider how the variation of PTX conditions in the hydrothermal system can modify the composition of the separated vapour. Computations performed with the LONER AP code (http://fluids.unileoben.ac.at) indicate that, by fixing bulk composition and pressure, a temperature decrease would be paralleled by a decrease of the steam fraction and consequent increase of χCO_2

in the vapour phase. Otherwise, an increase of CO_2 in the bulk fluid, at constant pressure and temperature, would induce an increase of the steam fraction, while χCO_2 in the vapour phase would remain almost unchanged. If pressure is not constrained, an increase of CO_2 in the bulk fluid, at constant temperature and steam fraction, would produce an increase of χCO_2 in the vapour phase. This implies that PTX conditions of the hydrothermal system needs to be accurately evaluated in order to get insights about eventual changes in the composition of shallow fluids. In particular, both temperature and fCO_2 , inferred from chemical composition of collected fluids, provide useful additional constraints.

Conclusions

Several thermal features emerge on the flanks of Nevado del Ruiz, namely thermal springs, streams, rivers, fumaroles. Presented data suggest that these manifestations discharge steam and gases coming from a hydrothermal system at temperature of about 315 °C. The presence of SO_2 in a low-temperature fumarole on the W flank of the volcano, and the mainly oxidising conditions observed in steam-heated waters, suggest that S-bearing gases are not fully equilibrated at hydrothermal reducing conditions, as testified by C-bearing gases, but recall magmatic conditions. This would imply that the hydrothermal system is still at an immature stage (as also suggested by the low pH), due to the continuous input of magmatic gases. Otherwise, full equilibrium among secondary minerals, gas and water would led to mature near-neutral high salinity brines.

The presence of oxidized S-bearing species both in the Nereidas fumarole and in steam-heated waters implies that an input of magmatic gases, although mixed with fluids of hydrothermal origin, is detectable even in the shallow parts of the hydrothermal system.

According to the results of the steam-heating model, it is possible to evaluate where the deep hydrothermal vapour is chiefly channelled, and eventually recompute, in the outline of systematic monitoring, the temporal variations in the flux of deep vapour in every single thermal manifestation. Among sampled steam-heated waters, the area of Hotel Thermales and Agua Caliente thermal springs are entered by the highest amount of deep vapour, with the highest estimated value of 20 l/s, and their composition is expected to closely track eventual variations of its flux.

According to the composition of the Nereidas fumarole, the PTX conditions of the hydrothermal reservoir has been estimated. The composition of Nereidas is compatible with a biphase system at 315°C, with a steam fraction of 0.46, at a pressure of 15MPa, having 10% wt of NaCl and 5% wt of CO_2. Changes in the chemical composition of the fumarole would provide insights on the fCO_2 of the reservoir, on its degree of vaporization, or its eventual pressurization. The eventual changes in the PTX conditions of the hydrothermal reservoir needs to be deeply evaluated to interpret correctly

any modification in the chemical composition of shallow fluid, by putting into the modellization the largest number of constraints. At the same time, the regular monitoring of the yield of streams and thermal springs, along with their chemical and isotope composition, would provide the key information on the amount of deep vapour condensing in the shallow thermal aquifer, thus getting insights on the present state of activity of the NdR volcano-hydrothermal system.

Appendix 1: Steam-water partition

The pristine hydrothermal and/or magmatic gas is thought to partially condense during ascent upon cooling. As an effect of partial condensation, the gas chemistry and water isotope composition can be modified according to the specific steam-water partition coefficient of every gas species and isotope enrichment factors.

Therefore, the following relationship holds for CO_2, H_2S, SO_2, CH_4 and HCl:

$$m_v = m_l \cdot B \qquad \text{A1)}$$

where m_v and m_l are the concentrations (in mol/kg_{H_2O}) in the vapor and liquid phases, and B is the partition coefficient expressed as $\frac{(\chi)_v}{(\chi)_l}$.

The following relation holds for isotopes:

$$\delta_l = \delta_v + \varepsilon_{l-v} \qquad \text{A2)}$$

where $\varepsilon_{l\text{-}v}$ is the isotope enrichment factor between liquid water and vapor.

The choice of appropriate partition coefficients and isotope-fractionation factors requires a careful assessment and specific assumptions. Concerning stable isotopes, the fractionation factor between liquid water and steam is computed at different temperatures based on the data obtained for pure water by Horita and Wesolovski (1994) and for saline water by Horita et al. (1995).

The partition coefficients for CO_2, CH_4, H_2S, SO_2 and HCl are dependent on hydrolysis reactions and consequent speciation in water. Therefore, the solution pH and f_{O_2}, in addition to temperature, must be considered in order to account for the effective solubilities of these species. A major problem arises for sulfur speciation during steam separation and condensation in water. Oxygen fugacity and pH critically affect the calculation of sulfur speciation, and that in liquid water is represented by the redox-dependent species SO_4^{2-}, HSO_4^-, H_2S_{aq}, HS^-, S^{--}, SO_{2aq}, HSO_3^- and SO_3^{2-}. As a consequence, the apparent solubility constant must take into account the hydrolysis of sulfur-bearing gases, and pH and redox conditions must be constrained. Redox potential measured in steam-heated waters is quite oxidizing, and average log fO_2 is close to the buffer SO_2-H_2S-0.5 at

60°C (-52.4). Solution pH is very acidic, and is fixed at 1 pH units. We assume that in the shallow steam-heated aquifer, redox conditions are not controlled by minerals (due to very immature gas-water-rock equilibrium) but still by the gas phase. Partial condensation of the vapour emitted from Nereidas, instead, would occur at more reducing conditions, i.e. those fixed by measured H_2/H_2O ratios, in equilibrium with hydrothermal conditions ($FeO\text{-}Fe_2O_3$ buffer), whilst pH=6 is assumed, according to the value measured in Nereidas w., a stream fed by the condensed vapour.

The S_{tot} content in thermal water, in general, is given by

$$S_{TOT} = SO_4^{2-} + HSO_4^- + HSO_3^- + SO_3^{2-} + H_2S_{aq} + HS^- + S^{2-} + SO_{2,aq} \quad \text{A3)}$$

Of course, only few of these species will be significant in considered solutions, depending on pH and fO_2. The apparent solubility constant is derived from the following equilibria, governed by the respective constants (Johnson et al., 1992):

$$H_2S_{aq} + 2\,fO_2 = 2H^+ + SO_4^{--} \qquad K_{1,S} \qquad \text{A4)}$$

$$HS^- + 2\,fO_2 = H^+ + SO_4^{2-} \qquad K_{2,S} \qquad \text{A5)}$$

$$S^{2-} + 2\,fO_2 = SO_4^{--} \qquad K_{3,S} \qquad \text{A6)}$$

$$SO_{2,aq} + 0.5\,fO_2 = 2H^+ + SO_4^{2-} \qquad K_{4,S} \qquad \text{A7)}$$

$$HSO_3^- + 0.5\,fO_2 = H^+ + SO_4^{2-} \qquad K_{5,S} \qquad \text{A8)}$$

$$SO_3^{2-} + 0.5\,fO_2 = SO_4^{2-} \qquad K_{6,S} \qquad \text{A9)}$$

$$HSO_4^- = H^+ + SO_4^{2-} \qquad K_{7,S} \qquad \text{A10)}$$

$$fH_2S + 2\,fO_2 = 2H^+ + SO_4^{2-} \qquad K_{8,S} \qquad \text{A11)}$$

$$fSO_2 + H_2O + 0.5\,fO_2 = 2H^+ + SO_4^{2-} \qquad K_{9,S} \qquad \text{A12)}$$

By combining together the first seven equilibria and referring to Equation A3, we obtain the

$$m_{S_{TOT}} = m_{SO_4^{2-}} \cdot \left(1 + \frac{a_{H^+}}{fO_2^2 K_{2,S}} + \frac{1}{fO_2^2 K_{3,S}} + \frac{a_{H^+}^2}{fO_2 K_{1,S}} + \frac{a_{H^+}}{fO_2^{0.5} K_{5,S}} + \frac{1}{fO_2^{0.5} K_{6,S}} + \frac{a_{H^+}^2}{fO_2^{0.5} K_{4,S}} + \frac{a_{H^+}}{K_{7,S}}\right) =$$

$m_{SO_4^{2-}} \cdot B$.

By substituting $m_{SO_4^{2-}} = \frac{m_{S_{TOT}}}{B}$ in reactions K8 and K9 we obtain $H_2S_v = S_{TOT,aq}$ and $SO_{2v} = S_{TOT,aq}$ equilibria:

$$fH_2S = \frac{a_{H^+}^2}{fO_2^{\ 2} \cdot K_{8,S}} \cdot \frac{m_{S_{TOT,aq}}}{B} = m_{S_{TOT,aq}} \cdot K^*_{H,H_2S} \qquad \text{A13)}$$

$$fSO_2 = \frac{a_{H^+}^2}{fO_2^{\ 0.5} K_{9,S}} \cdot \frac{m_{S_{TOT,aq}}}{B} = m_{S_{TOT,aq}} \cdot K^*_{H,SO_2} \qquad \text{A14)}$$

It can be easily obtained that the molal concentration of S species in the vapor phase is

$$m_{H_2S,v} = m_{S_{TOT}} K^*_{H,H_2S} \cdot \frac{55.55}{P_{H_2O}} \qquad \text{A15)}$$

$$m_{SO_2,v} = m_{S_{TOT}} K^*_{H,SO_2} \cdot \frac{55.55}{P_{H_2O}} \qquad \text{A16)}$$

Analogously, the solubility of CO_2 is essentially governed by hydrolysis, based on the following equations, valid for acidic pH:

$$CO_{2,aq} + H_2O = H^+ + HCO_3^- \qquad K_{1,C} \qquad \text{A17)}$$

$$fCO_2 + H_2O = H^+ + HCO_3^- \qquad K_{2,C} \qquad \text{A18)}$$

$$C_{TOT} = HCO_3^- + CO_3^{2-} + CO_{2,aq} \qquad \text{A19)}$$

By combining these two reactions, we obtain the following expression for the $CO_{2g} = C_{TOT,aq}$ equilibrium:

$$f_{CO_2} = \frac{a_{H^+}}{K_{2,C}} \cdot \frac{m_{C_{TOT,aq}}}{\left(1 + \frac{a_{H^+}}{K_{1,C}}\right)} = m_{C_{TOT,aq}} \cdot K^*_{H,C} \qquad \text{A20)}$$

The molal concentration of CO_2 in the vapor phase then becomes

$$m_{CO_2,v} = m_{C_{TOT,aq}} K^*_{H,C} \cdot \frac{55.55}{P_{H_2O}} \qquad \text{A21)}$$

Concerning CH_4, similar reactions hold

$$CH_{4,aq} + 2O_2 = H^+ + H_2O + HCO_3^- \qquad K_{1,CH} \qquad \text{A22)}$$

$$fCH_4 + 2O_2 = H^+ + H_2O + HCO_3^- \qquad K_{2,CH} \qquad \text{A23)}$$

$$C_{TOT} = HCO_3^- + CO_3^{2-} + CH_{4,aq} \qquad \text{A24)}$$

By combining these two reactions, we obtain the following expression for the $CH_{4g} = C_{TOT,aq}$ equilibrium:

$$f_{CH_4} = \frac{m_{C_{TOT,aq}}}{\left(1 + K_{1,C} \cdot \frac{fO_2^2}{a_{H^+}}\right) K_{2,C}} = m_{C_{TOT,aq}} \cdot K^*_{H,C} \qquad \text{A25)}$$

The molal concentration of CH_4 in the vapor phase then becomes

$$m_{CH_{4,v}} = m_{C_{TOT,aq}} K^*_{H,CH} \cdot \frac{55.55}{P_{H_2O}} \qquad \text{A26}$$

Finally, HCl solubility strongly depends on the rapid hydrolysis of HCl, based on the following equilibria:

$$HCl_g = Cl^- + H^+ \qquad K_{1,HCl} \qquad \text{A27}$$

$$HCl_{aq} = Cl^- + H^+ \qquad K_{2,HCl} \qquad \text{A28}$$

$$Cl_{TOT} = Cl^- + HCl_{aq} \qquad K_{3,HCl} \qquad \text{A29}$$

The concentration of HCl in the vapor phase becomes

$$f_{HCl} = \frac{m_{Cl_{TOT,aq}}}{\left(1 + \frac{K_{2,HCl}}{a_{H^+}}\right) \cdot K_{1,HCl} K_{2,HCl}} = m_{Cl_{TOT,aq}} \cdot K^*_{H,HCl} \qquad \text{A30}$$

and the molal concentration in the vapor phase is

$$m_{HCl,v} = m_{Cl_{TOT,aq}} K^*_{H,HCl} \cdot \frac{55.55}{P_{H_2O}} \qquad \text{A31}$$

Captions

Figure 2 - Cl-SO_4-C_{tot} triangular diagram. The fields of chloride, steam-heated and perypheral waters are also shown.

Figure 3 - pH-TDS scatter plot for collected thermal waters.

Figure 4 - δD-$\delta^{18}O$ scatter plot of collected thermal waters. The GMWL is plotted as reference. The model curves represent the composition of a steam-heated water for increasing amount of condensing deep steam. Red crosses represent different ϕ/σ ratios. The red diamond represents the isotope composition of the deep steam, before condensation into the shallow aquifer, whilst the red circle is the composition of the 250°C undiluted fluid, as retrieved from Botero Londono and Rio Molinos mixing model (dashed line). See text for details.

Figure 5 - CH_4-N_2-CO_2 triangular diagram for gases dissolved in thermal waters. The composition of few samples from crater fumaroles (Giggenbach et al., 1990) are reported for comparison. Measured compositions plot in the field between hydrothermal and atmospheric gases.

Figure 6 - Relative Na, K, Mg of thermal waters. Isotherms curves and the fields of immature waters and full equilibrium are taken from Giggenbach (1988).

Figure 7 - a) Saturation index with respect to selected minerals, computed at different temperatures for Botero Londono with the PHREEQCI code; b) Saturation index with respect to selected

minerals, computed at different temperatures for the undiluted water, as retrieved from Botero Londono and Rio Molinos mixing model (see text for details).

Figure 8 - CO-CO_2-CH_4 scatter plot for gases dissolved in thermal waters.

Figure 9 - Log(CO/CO_2)-Log(CH_4/CO_2) scatter plot for gases dissolved in thermal waters. The buffer FeO-Fe_2O_3 is also plotted (*vapour*), along with the curve representing the full equilibrium in a liquid phase (*liquid*) at the fO_2 fixed by the buffer. The fH_2O is fixed by the boiling of a brine according to equation 4 (Giggenbach, 1980). Dotted lines represents different fraction of condensation at various temperature, following the model by Chiodini ad Marini (1998).

Figure 10 - a) SO_4-Cl scatter plot for thermal waters; the model curves represent the composition of a steam-heated water for increasing amount of condensing deep steam; red crosses represent different ϕ/σ ratios, the black dot is the composition of the deep vapour, fitting with the model, the red dot is the composition of the deep vapour, resulting from equilibrium computions (see text for explanation). b) $\delta^{18}O$-Cl scatter plot for thermal waters; model curves as in Figure 10a.

Figure 11 - Portion of the H_2O-CO_2-NaCl ternary diagram, representing PTX conditions for the modelled hydrothermal system. The range of composition of the bulk fluid is plotted as red thick line, along with the composition of the vapour and the liquid phases.

Table 1 - Temperature, pH, major ion composition, isotope composition of collected thermal waters. The mass output rate of thermal waters (Q) and the deep vapour (ϕ) as computed from the steam-heating model (see text for details).

Table 2 - Chemical composition of Nereidas fumarolic vapour and gases dissolved in thermal waters. Stable isotope of the Nereidas fumarole condensate were measured on a sample collected in October 2013.

Table 3 - Temperature, pH and chemical composition of the undiluted parent water recomputed from Botero Londono.

Table 4 - Initial and boundary conditions for the steam-heating model.

Table 5 - Initial and boundary conditions for the computation of PTX conditions of the hydrothermal reservoir by means of LONER AP software, and computed composition of the vapour and liquid phases.

Table 6 - a) Equilibrium composition of the vapour and liquid phases computed by means of HSC 6.1 code; species with molal contents below 10^{-7} are neglected ; b) equilibrium composition of the vapour, solid and liquid phases.

Acknowledgement

This work has been supported by the Servicio Geologico Colombiano for field campaigns and logistics. The Authors wish to thank the AGC staff for scientific discussions about the NRV activity.

References

Alfaro, C. M., Gil, R. A., Osorio, F., & Jairo, A. Descarga de SO2 a la atmósfera desde el volcan Nevado del Ruiz. In 2o. Simposio Internacional de Geoquímica Ambiental en Países Tropicales, Cartagena (Colombia). 21-25 Nov 1996. Geoquímica ambiental en países tropicales; memoria sp. 127-134 (No. Doc. 18414) CO-BAC, Bogotá).

Alvaro, H., Nieto, E., Brandsdóttir, B., & Muñoz, F. (1990). Seismicity associated with the reactivation of Nevado del Ruiz, Colombia, July 1985–December 1986. Journal of Volcanology and Geothermal Research, 41(1), 315-326.

Anderko A. and Pitzer K. S. , 1993. Equation of state representation of phase equilibria and volumetric properties of the system NaCl-H2O above 573 K. Geochim. Cosmochim. Acta 57, 1657–1680.

Arango EE, Buitrago A J, Cataldi R, Ferrara GC, Panichi C, Villegas VJ (1970) Preliminary study on the Ruiz Geothermal Project (Colombia). Geothermics, Special Issue 2:43-56

Badalamenti, B., Chiodini, G., Cioni, R., Favara, R., Francofonte, S., Gurrieri, S., ... & Nuccio, P. M. (1991). Special field workshop at Vulcano (Aeolian Islands) during summer 1988: geochemical results. Acta Vulcanol, 1, 223-227.

Bakker, R. J. (2003). Package FLUIDS 1. Computer programs for analysis of fluid inclusion data and for modelling bulk fluid properties. Chemical Geology, 194(1), 3-23.

Barberi F., Martini M. and Rosi M., 1990. Nevado del Ruiz (Colombia): pre-eruption observations and the November 13, 1985 catastrophic event. In: S.N. Williams (Editor), Nevado del Ruiz Volcano, Colombia, II. J. Volcanol. Geotherm. Res., 42: 1-12.

Calvache, M. L. V. (1990). Pyroclastic deposits of the November 13, 1985 eruption of Nevado del Ruiz volcano, Colombia. Journal of Volcanology and Geothermal Research, 41(1), 67-78.

Capasso, G., Favara, R., Grassa, F., Inguaggiato, S., and Longo, M., 2005, On-line technique for preparing and measuring stable carbon isotope of total dissolved inorganic carbon in water sample (□13CTDIC): Annals of Geophysics, v. 48, p. 159-166.

Capasso, G. and Inguaggiato, S., 1998, A simple method for the determination of dissolved gases in natural waters: An application to thermal waters from Vulcano island.: Applied Geochem., v. 13, p. 631-642.

Chiodini G. and Marini L., 1998. Hydrothermal gas equilibria: The H2O-H2-CO2-CO-CH4 system. Geochim. Cosmochim. Acta, 62, 15, 2673–2687.

Federico, C., Capasso, G., Paonita, A., Favara, R., 2010. Effects of steam-heating processes on a stratified volcanic aquifer: stable isotopes and dissolved gases in thermal waters of Vulcano Island (Aeolian archipelago). J. Volcanol. Geotherm. Res. 192, 178–190. http://dx.doi.org/10.1016/j.jvolgeores.2010.02.020.

Forero, J., Zuluaga, C., & Mojica, J. (2011). Alteration related to hydrothermal activity of the Nevado del Ruiz Volcano (NRV), Colombia. Boletín de Geología, 33(1), 59-67.

García-Cano, L. C., Castaño, K. P., García, M. E., Cruz, F. G., Acevedo, A. P., Londoño, J. M., ... & Osorio, 2011. J. MUESTREO DE LA ACTIVIDAD SÍSMICA EN EL SECTOR HONDA-PULI, VALLE MEDIO DEL MAGDALENA, COLOMBIA.

Giggenbach, W. F. (1975). A simple method for the collection and analysis of volcanic gas samples. Bulletin volcanologique, 39(1), 132-145.

Giggenbach, W.F., 1980. Geothermal gas equilibria. Geochim. Cosmochim. Acta 44, 2021–2032.

Giggenbach, W.F., 1988. Geothermal solute equilibria. Derivation of Na-K-Mg-Ca geoindicators. Geochim. Cosmochim. Acta 52, 2749-2765.

Giggenbach, W.F., Garcia, P.N., Londono, C.A., Rodriguez, V.L.A., Rojas, G.N. and Calvache V.M.L., 1990. The chemistry of fumarolic vapor and thermal-spring discharges from the Nevado del Ruiz volcanic-magmatic-hydrothermal system, Colombia. In: S.N. Williams (Editor), Nevado del Ruiz Volcano, Colombia, II. J. Volcanol. Geotherm. Res., 42, 13-39.

Herd, D. G. (1982). Glacial and volcanic geology of the Ruiz--Tolima volcanic complex, Cordillera Central, Colombia (No. 8). Instituto Nacional de Investigaciones Geológico-Mineras.

Horita, J., Wesolowski, D.J., 1994. Liquid-vapor fractionation of oxygen and hydrogen isotopes of water from the freezing to the critical temperature. Geochim. Cosmochim. Acta 58, 3425–3437.

Horita, J., Cole D.R., Wesolowski, D.J. (1995) The activity-composition relationship of oxygen and hydrogen isotopes in aquesous salt solutions: III. Vapor-liquid water equilibration of NaCl solutions to 350°C. Geochim. Cosmochim. Acta, 59, 6, 1139-1151.

HSC Chemistry 6.1® , 2008. Chemical Reaction and Equilibrium Software with Thermochemical Database and Simulation Module. Oututec Research Oy, Pori.

Inguaggiato, C., Censi, P., Zuddas, P., Londoño, J., M., Chacón, Z., Alzate, D, Brusca, L., D'Alessandro, W. 2015. Geochemistry of REE, Zr and Hf in a wide range of pH and water composition: The Nevado del Ruiz volcano-hydrothermal system (Colombia). Chem. Geol. 417, 125-133.

Johnson, J., Oelkers, E., Helgeson, H., 1992. SUPCRT92: a software package for calculating the standard molal thermodynamic properties of minerals, gases, aqueous species and reactions from 1 to 5000 bar and 0 to 1000 °C. Computational Geosciences 18, 899–947.

Krueger, A. J., Walter, L. S., Schnetzler, C. C., & Doiron, S. D. (1990). TOMS measurement of the sulfur dioxide emitted during the 1985 Nevado del Ruiz eruptions. Journal of Volcanology and Geothermal Research, 41(1-4), 7-15.

Larson, P.B. and Taylor, H.P., 1986. An oxygen isotope study of hydrothermal alteration in the Lake-City Caldera, San-Juan Mountains, Colorado. J. Volcanol. Geotherm. Res. 30, 47-82.

Liotta, M., Paonita, A., Caracausi, A., Martelli, M., Rizzo, A., & Favara, R. (2010). Hydrothermal processes governing the geochemistry of the crater fumaroles at Mount Etna volcano (Italy). Chemical Geology, 278(1), 92-104.

Londoño, J. M. (2010a). ASPECTOS RELEVANTES DE LA ACTIVIDAD DEL VOLCáN NEVADO DEL RUIz. 1985-2008. Glaciares, nieves y hielos de América Latina. Cambio climático y amenazas, 261.

Londoño, B., & Makario, J. (2010b). Activity and Vp/Vs ratio of volcano-tectonic seismic swarm zones at Nevado del Ruiz volcano, Colombia. Earth Sciences Research Journal, 14(1), 111-124.

Martinelli, B. (1990). Analysis of seismic patterns observed at Nevado del Ruiz volcano, Colombia during August–September 1985. Journal of Volcanology and Geothermal Research, 41(1-4), 297-314.

Mejía, E. L., Velandia, F., Zuluaga, C. A., López, J. A., & Cramer, T. (2012). ANÁLISIS ESTRUCTURAL AL NORESTE DEL VOLCÁN NEVADO DEL RUÍZ, COLOMBIA–APORTE A LA EXPLORACIÓN GEOTÉRMICA. Boletín de Geología, 34(1), 27-41.

Naranjo, J. L., Sigurdsson, H., Carey, S. N., & Fritz, W. (1986). Eruption of the Nevado del Ruiz volcano, Colombia, on 13 November 1985: tephra fall and lahars. Science, 233(4767), 961-963.

Parkhurst, D.L. and Appelo, C.A.J., 1999. User's guide to PHREEQC (version 2)--A computer program for speciation, batch-reaction, one-dimensional transport, and inverse geochemical calculations: U.S. Geological Survey Water-Resources Investigations Report 99-4259, 312 p.

Parra, E., & Cepeda, H. (1990). Volcanic hazard maps of the Nevado del Ruiz volcano, Colombia. Journal of Volcanology and Geothermal Research, 42(1-2), 117-127.

Reed, M.H., Spycher, N.F., 1984. Calculation of pH and mineral equilibria in hydrothermal waters with application to geothermometry and studies of boiling and dilution. Geochim. Cosmochim. Acta 48, 1479–1492.

Sano, Y., Wakita, H., & Williams, S. N. (1990). Helium-isotope systematics at Nevado del Ruiz volcano, Colombia: implications for the volcanic hydrothermal system. Journal of Volcanology and Geothermal Research, 42(1), 41-52.

Seewald, J.S., Zolotov, M.Y. and McCollom, T, 2006. Experimental investigation of single carbon compounds under hydrothermal conditions. Geochim. Cosmochim. Acta 70, 446–460.

Shock, E.L., Holland, M., Meyer-Dombard, D., Amend, J.P., Osburn, G.R. and Fischer, T.P., 2010. Quantifying inorganic sources of geochemical energy in hydrothermal ecosystems, Yellowstone National Park, USA. Geochim. Cosmochim. Acta 74, 4005–4043.

F. Sortino, S. Inguaggiato, S. Francofonte (1991). Determination of HF, HCl, and total sulfur in fumarolic fluids by ion chromatography. Acta Vulcanol., 1, pp. 89–91.

Spycher, N.F. and Reed, M.H., 1988. Fugacity coefficients of H2, CO2, CH4, H2O and of H2O-CO2-CH4 mixtures: A virial equation treatment for moderate pressures and temperatures applicable to calculations of hydrothermal boiling. Geochim. Cosmochim. Acta 52, 739-749.

Stix, J., Layne, G. D., & Williams, S. N. (2003). Mechanisms of degassing at Nevado del Ruiz volcano, Colombia. Journal of the Geological Society, 160(4), 507-521.

Sturchio, N.C., Williams, S.N., Garcia, N.P., Londono, A.C., 1988. The hydrothermal system of Nevado del Ruiz volcano, Colombia. Bull Volcanol 50, 399-412.

Thouret, J. C. (1990). Effects of the November 13, 1985 eruption on the snow pack and ice cap of Nevado del Ruiz volcano, Colombia. Journal of Volcanology and Geothermal Research, 41(1-4), 177-201.

Uruena-Suarez, C.L., Zuluaga, C.A. and Molano, J.C., 2012. Estudio de inclusiones fluidas en pozos de gradiente térmico, volcán Nevado del Ruiz. Bol. Geol., 34, 2, 103-115.

Wagner, W., Overhof, U., 2006. Extended IAPWS-IF97 Steam tables, Version 2.0, 2006, CD-ROM., Jewel case ISBN: 978-3-540-21412-0. Elsevier.

White, A.F., Chuma, N.J., and Goff, F., 1992. Mass-transfer constraints on the chemical evolution of an active hydrothermal system, Valles Caldera, New Mexico. J. Volcanol. Geotherm. Res., 49, 233-253.
Williams, S. N., Sturchio, N. C., Mendez, R., Londoño, A., & García, N. (1990). Sulfur dioxide from Nevado del Ruiz volcano, Colombia: total flux and isotopic constraints on its origin. Journal of Volcanology and Geothermal Research, 42(1-2), 53-68.

Table 1

Click here to download Table: Table1.xls

Sample Name	Date	type	T	pH	Eh	Na	K	Mg	Ca	Cl	SO_4	HCO_3
			°C		mV	mg/l						
Agua Hedionda	10/19/2013	bicarbonate	13.9	5.5	60	11	3	26	30	2	96	140
Nereidas w.	10/21/2013	bicarbonate	50.4	6.1	30	123	18	47	130	22	298	573
Rio Molinos	10/8/2013	bicarbonate	15.9	8.8	-90	47	8	15	57	51	173	73
Rio Lagunillas	10/19/2013	sulfate steam-heated	6.8	3.6	170	4	1	7	17	3	134	0
Rio Gualì	9/26/2013	sulfate steam-heated	7.2	3.5		24	6	30	108	27	553	0
Rio Azufrado	10/16/2013	sulfate steam-heated	16	3.4	190	106	15	113	265	55	1548	0
FT Gualì	10/18/2013	sulfate steam-heated	59.2	2.8	250	42	11	70	348	46	1509	0
Termal La Gruta	10/18/2013	sulfate steam-heated	33.5	3.1	240	323	55	144	177	513	3541	0
Hotel 1	9/26/2013	sulfate steam-heated	59.7	1.2	15	481	70	224	242	736	4999	0
Hotel 2	9/26/2013	sulfate steam-heated	62.6	1.2	120	494	75	236	256	775	5399	0
Agua Caliente	10/12/2013	sulfate steam-heated	59.3	1.2	330	345	225	189	247	1266	10575	0
Quebrada La Gruta	10/21/2013	sulfate steam-heated	15.3	3.4	210	110	33	50	61	175	1206	0
Agua Blanca	9/26/2013	sulfate steam-heated	29.1	3.3	210	42	10	53	416	49	1541	0
Botero Londono	10/8/2013	chloride	79.5	7.7	-30	622	82	6	48	1007	65	85

Table 2

Click here to download Table: Table 2.xls

fumarole	*Date*	t	H_2O	CO_2	S_{tot}	HCl	CH_4	CO	H2	**δD**	**$\delta^{18}O$**
		°C				µmol/mol				‰	SMOW
Nereidas	9/3/16	80	696900	250000	52820	<70	30200	0.26	2290	-135.4	-21.2

dissolved gases

Sample name	H_2	O_2	N_2	CO	CH_4	CO_2	pH_2	pO_2	pN_2	pCO	pCH_4	pCO_2
			cc/l STP						atm			
Agua blanca		0.03	4.6	1.5E-05	1.3E-02	351		1.2E-03	0.33	7.5E-07	4.4E-04	0.51
Agua Calientes	2.6E-02	1.0	6.5	5.0E-03	3.6E-02	198	1.6E-03	5.4E-02	0.59	3.3E-04	1.8E-03	0.51
Agua Hedionda		0.1	9.0	2.3E-05	1.4E-02	182		3.0E-03	0.56	9.6E-07	3.8E-04	0.21
Botero Londono	2.4E-03	2.7	8.2	2.4E-04	4.6E-04	2	1.4E-04	1.6E-01	0.75	1.7E-05	2.5E-05	0.006
FT Guali	2.1E-03		7.7	2.7E-03	7.1E-04	83	1.3E-04		0.70	1.7E-04	3.5E-05	0.21
Hotel 1	1.4E-01		7.7	3.4E-03	5.9E-03	158	8.5E-03		0.70	2.2E-04	2.9E-04	0.41
Hotel 2	1.8E-01		5.6	4.0E-03	4.7E-03	125	1.1E-02		0.51	2.6E-04	2.3E-04	0.33
Nereidas			3.0	1.5E-04	4.9E-02	363			0.26	9.0E-06	2.2E-03	0.81
Rio Azufral			10.6	5.6E-05	1.7E-04	7			0.62	2.3E-06	4.4E-06	0.008
Rio Gauli			8.8	1.7E-05	1.5E-04	2			0.80	1.1E-06	7.2E-06	0.004
Rio Lagunillas		2.6	11.1	3.8E-05	2.0E-04	6		6.3E-02	0.55	1.3E-06	4.0E-06	0.004
Rio Molinos			13.4	4.7E-04	8.2E-04	197			0.78	1.8E-05	2.1E-05	0.19

Table 3

Click here to download Table: Table 3.xls

undiluted water - Botero	*Londono*
t (°C)	250
pH	6.94
	mg/l
CO_2	26
HCO_3^-	7
Ca^{+2}	10
Cl^-	2220
K^+	180
Na^+	1360
SiO_2	310

Table 4

Click here to download Table: Table 4.doc

steam-heated water

T°C	logfO_2	pH
100	-46.2	1.2

Cold meteoric recharge

T°C	δD	$\delta^{18}O$	S_{tot} mol/kg	Cl mol/kg
10	-99	-13.9	0.0005	0.003

Deep fumarolic vapour

δD	$\delta^{18}O$	S_{tot} mol/mol	HCl mol/mol
-88.4	-10.5	0.01	0.004

Table 5

Click here to download Table: Table 5.xls

Table 5		
t	315	°C
P	150	bar
y	0.46	
$[CO_2]_{bulk}$	2.3	% mol
$[NaCl]_{bulk}$	10	% wt
fCO_2	37	bar
vapour		
$\chi_{CO2,v}$	0.22	
$\chi_{H2O2,v}$	0.77	
$\chi_{NaCl,v}$	9.90E-07	
liquid		
$\chi_{CO2,l}$	0.005	
$\chi_{H2O,l}$	0.96	
$\chi_{NaCl,l}$	0.037	

Table 6

Click here to download Table: table 6 ab.xls

Table 6	*b*
t (°C)	315
P (bar)	150
y = 0.46	

vapour	χ	ϕ	*f* (bar)
$CO_{2(g)}$	0.27	1.18	48
$H_2O_{(g)}$	0.72	0.65	70
$H_{2(g)}$	4.8E-04	1	0.07
$HCl_{(g)}$	1.0E-03	1	0.15
$SO_{2(g)}$	1.1E-10	1	1.6E-08
$H_2S_{(g)}$	0.012	1.05	1.8
$NaCl_{(g)}$	4.1E-14	0.0013	7.95E-15
$CH_{4(g)}$	2.4E-04	1.03	0.04
log$f$ O_2	-32.1		

liquid	mg/kg	γ	*a*
H_2O	860000	0.99	0.92
$CH_{4(a)}$	3.2	1.00	3.9E-06
$CO_{2(a)}$	28400	1.20	0.015
HCO_3^-	0.001	0.46	1.1E-09
Cl^-	5930	0.41	0.001
Na^+	21300	0.37	0.007
$NaCl_{(a)}$	75900	0.36	0.009
HSO_4^-	2.1E-07	0.46	1.9E-14
HS^-	0.005	0.41	1.1E-09
$HCl_{(a)}$	1360	1.00	7.4E-04
$SO_{2(a)}$	0.02	1.00	5.7E-09
$H_2S_{(a)}$	2580	1.00	0.001
pH	4.9		

solid 9 mol/kg

	composition	
	input	equilibrium
Kaolinite	1	0
Albite	1	0
K-Feldspar	1	0

Figure 1

Click here to download Figure: Figure 1 .pdf

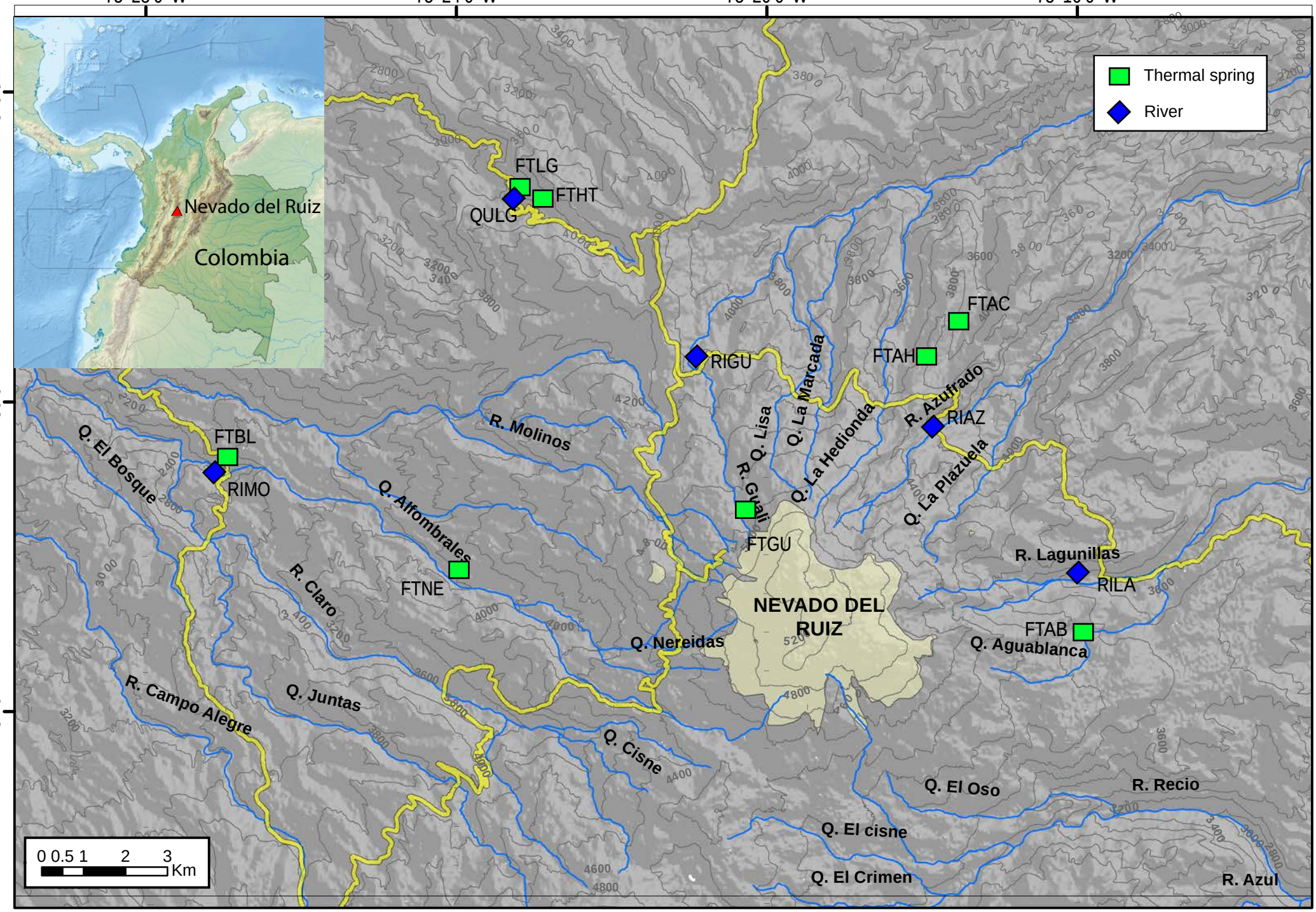

Figure 2
Click here to download Figure: Figure 2.pdf

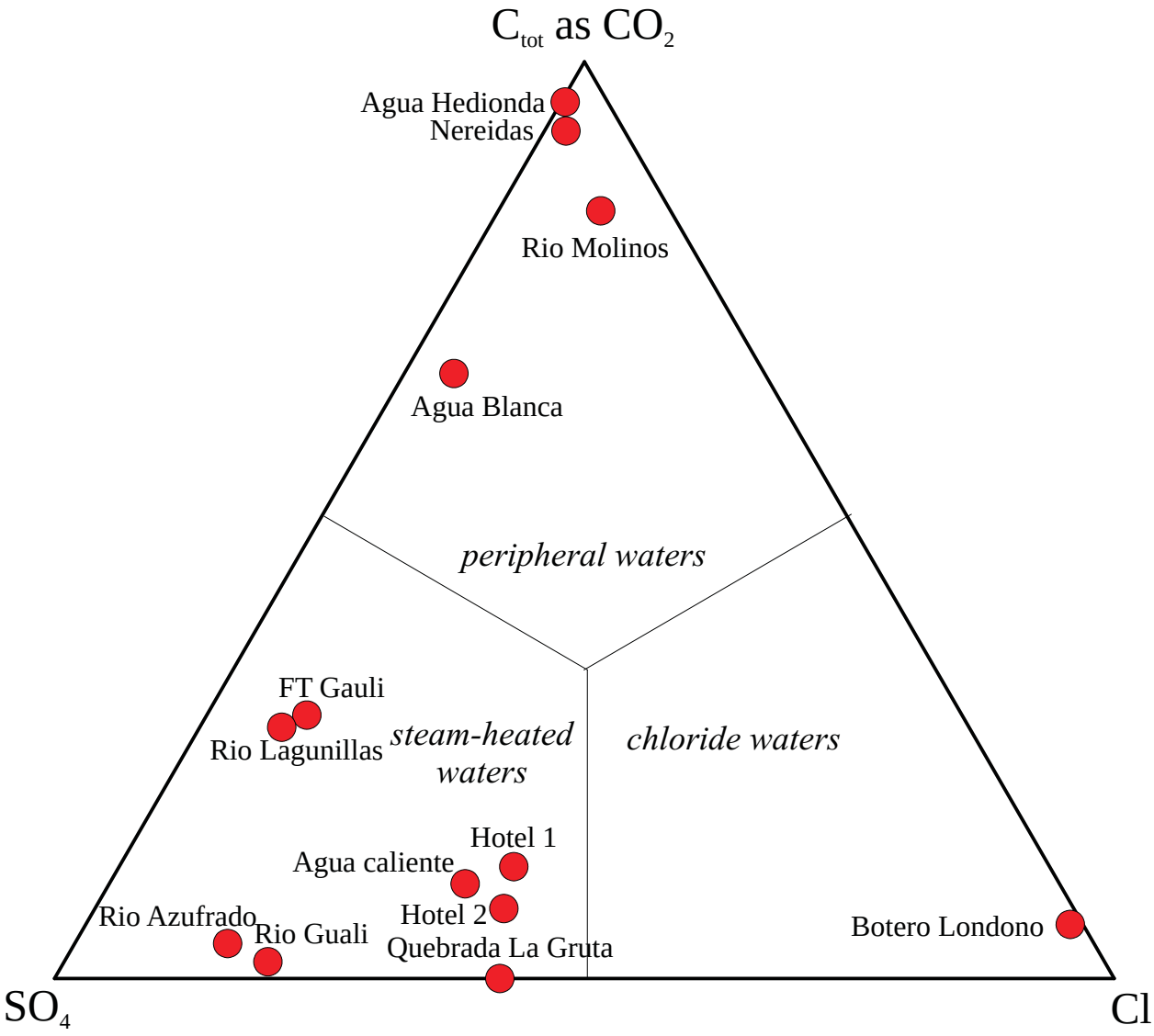

Figure 2

Figure 3
Click here to download Figure: Figure 3.pdf

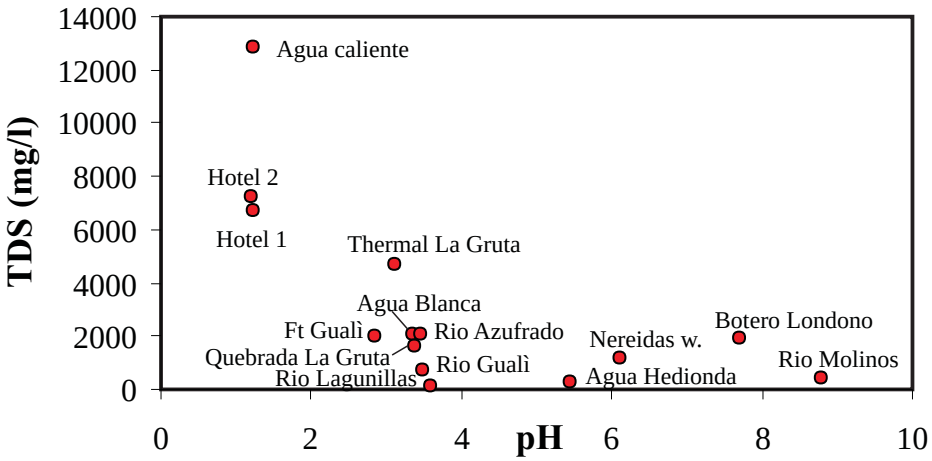

Figure 3

Figure 4

Click here to download Figure: Figure 4.pdf

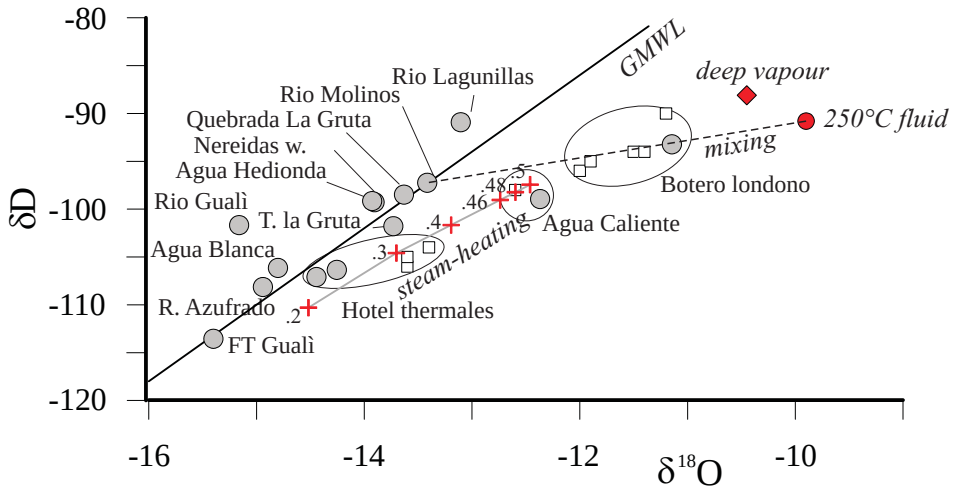

Figure 4

Figure 5
Click here to download Figure: Figure 5.pdf

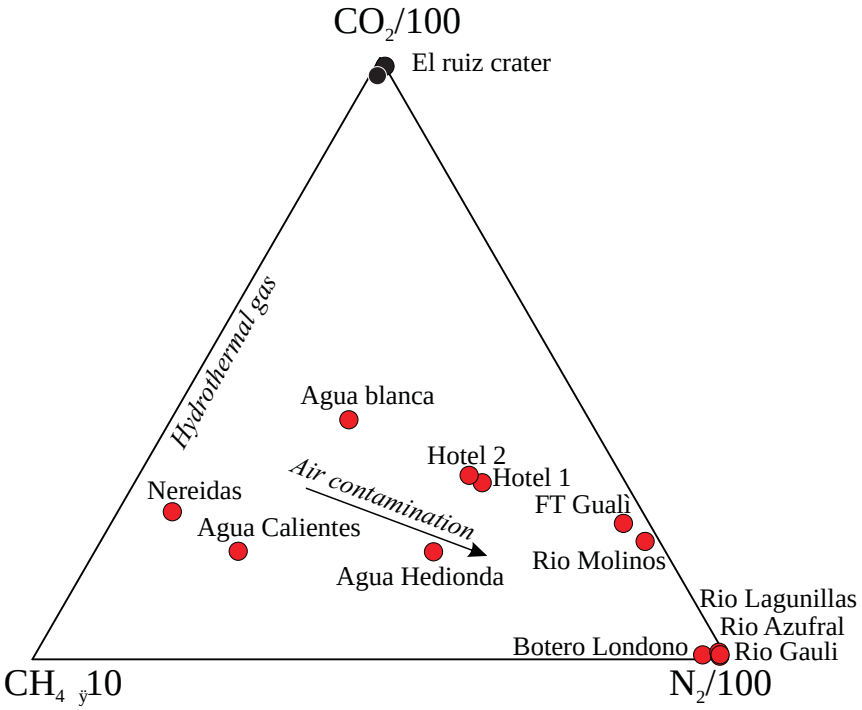

Figure 5

Figure 6
Click here to download Figure: Figure 6.pdf

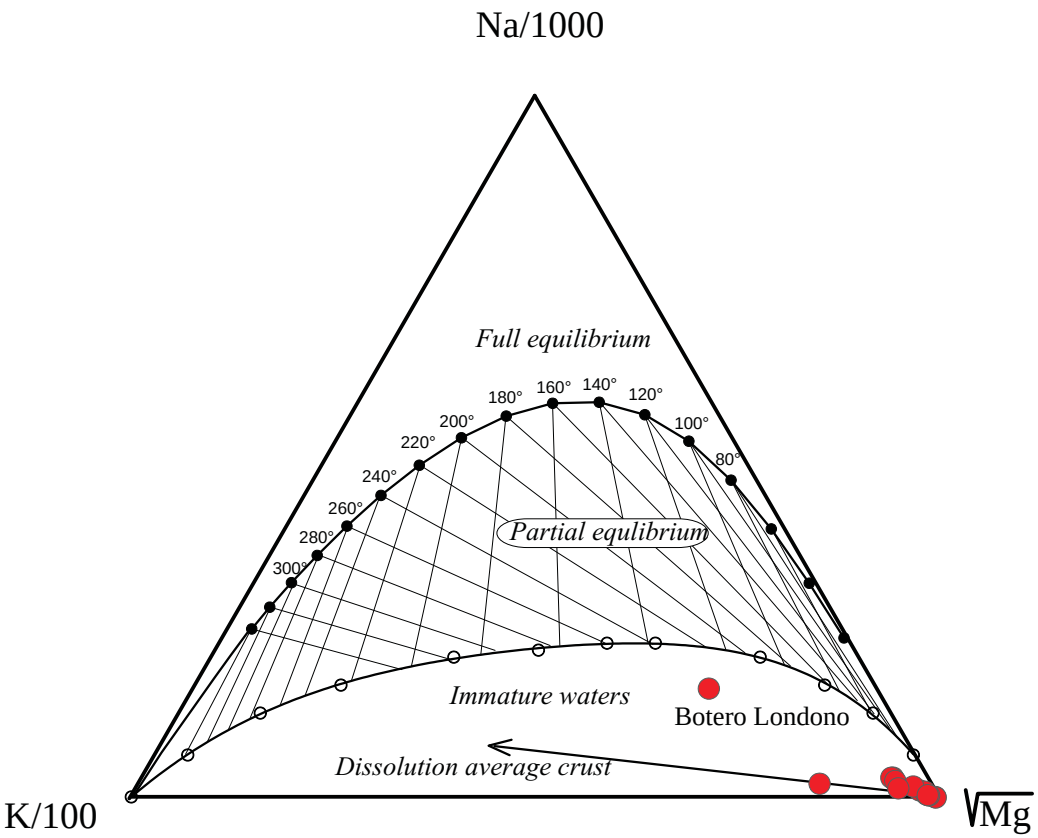

Figure 6

Figure 7
Click here to download Figure: Figure 7.pdf

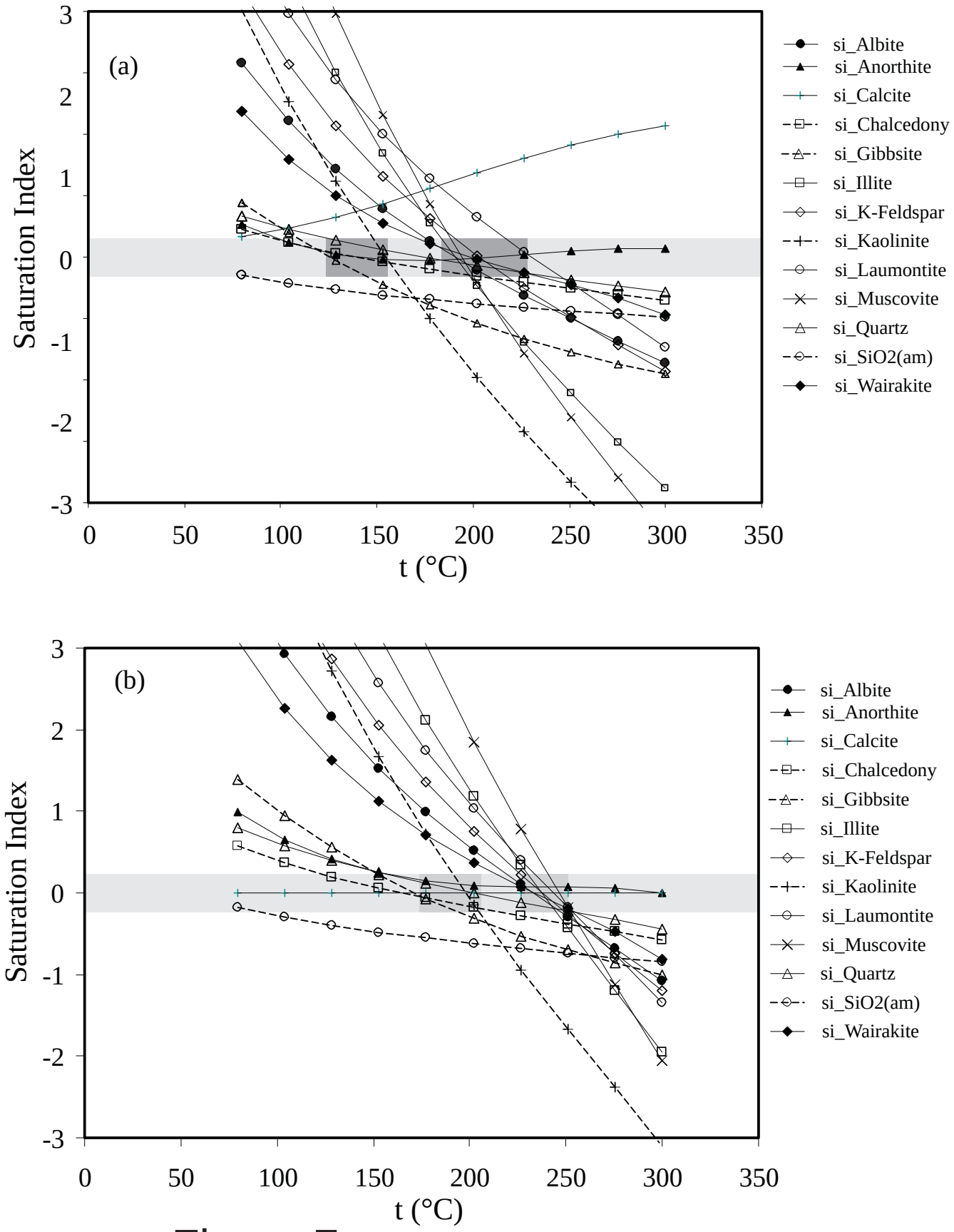

Figure 7

Figure 8
Click here to download Figure: Figure 8.pdf

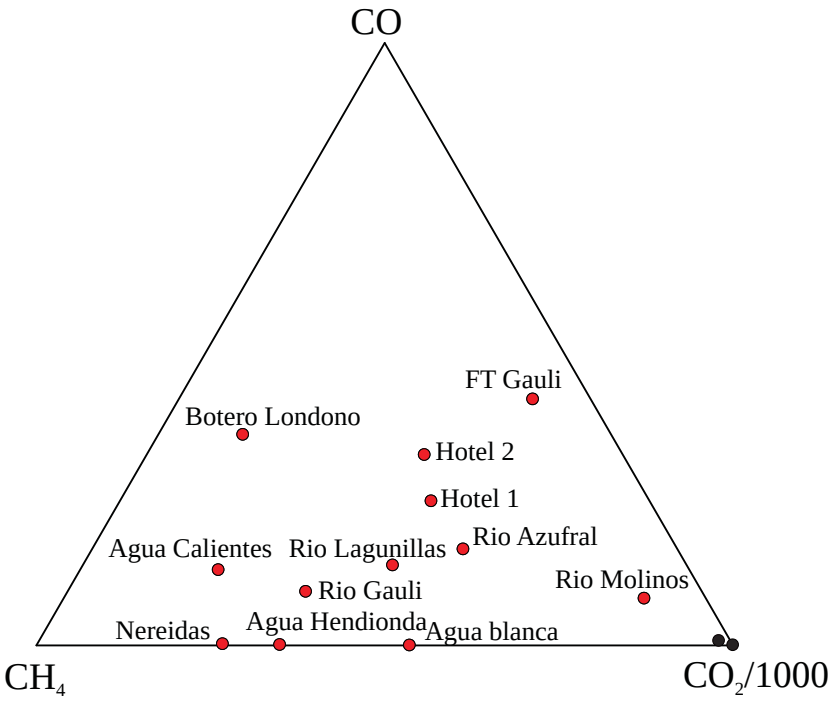

Figure 8

Figure 9

Click here to download Figure: Figure 9.pdf

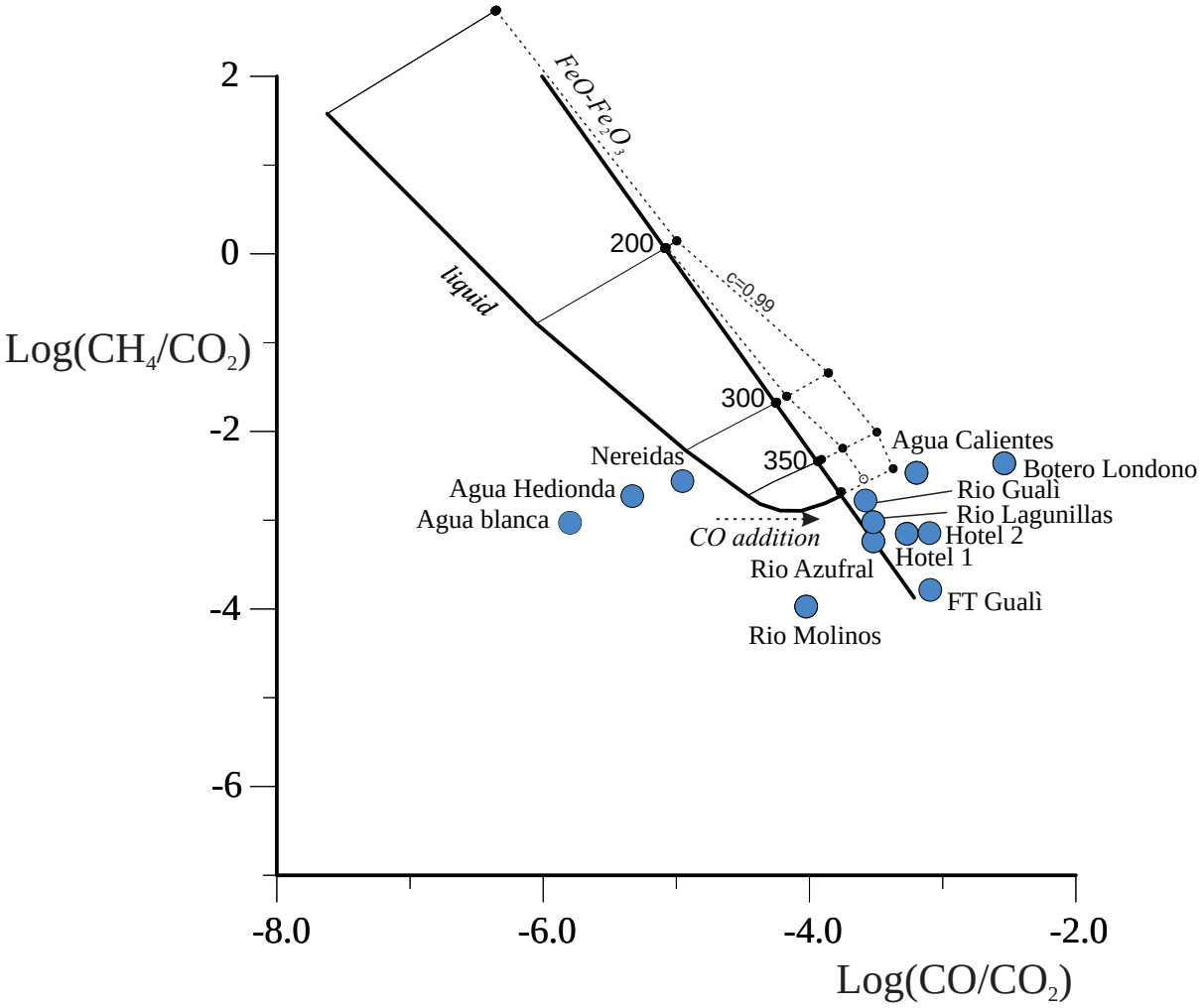

Figure 9

Figure 10
Click here to download Figure: Figure10.pdf

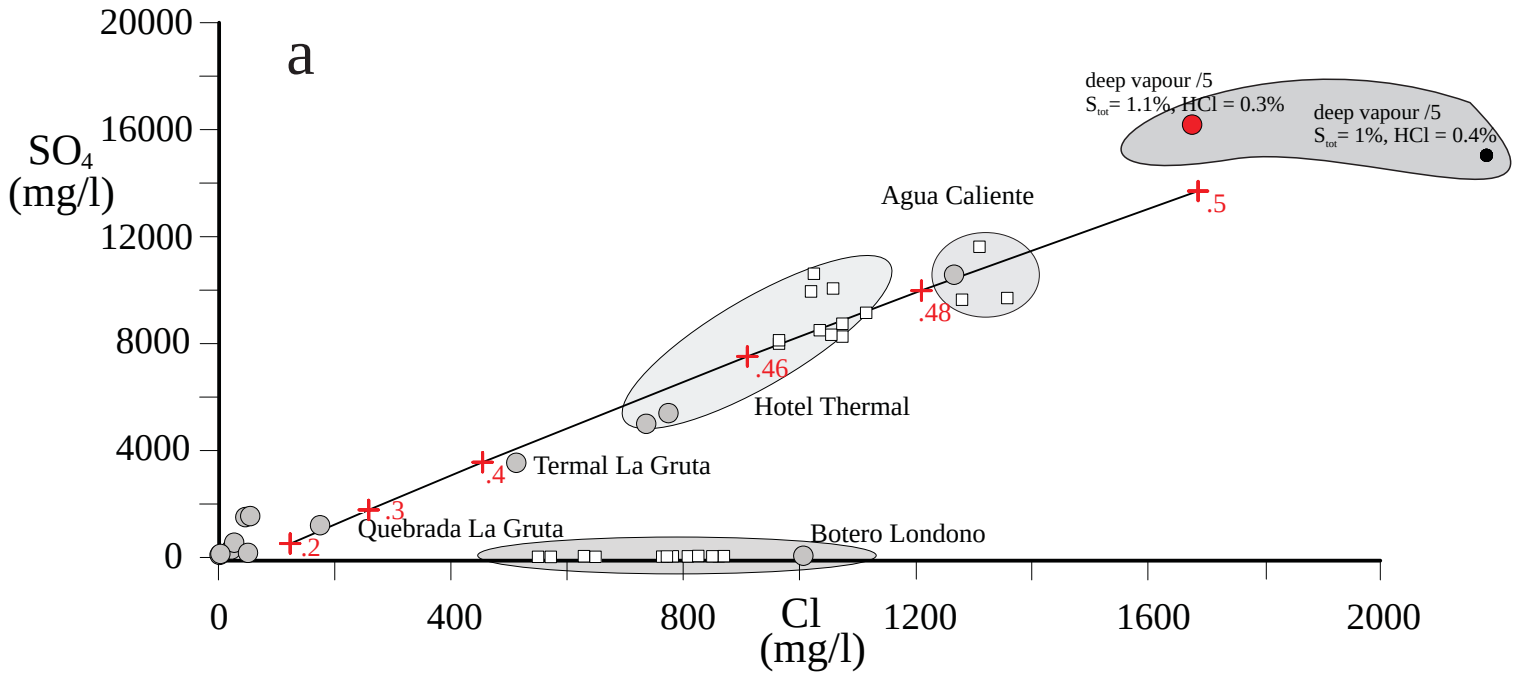

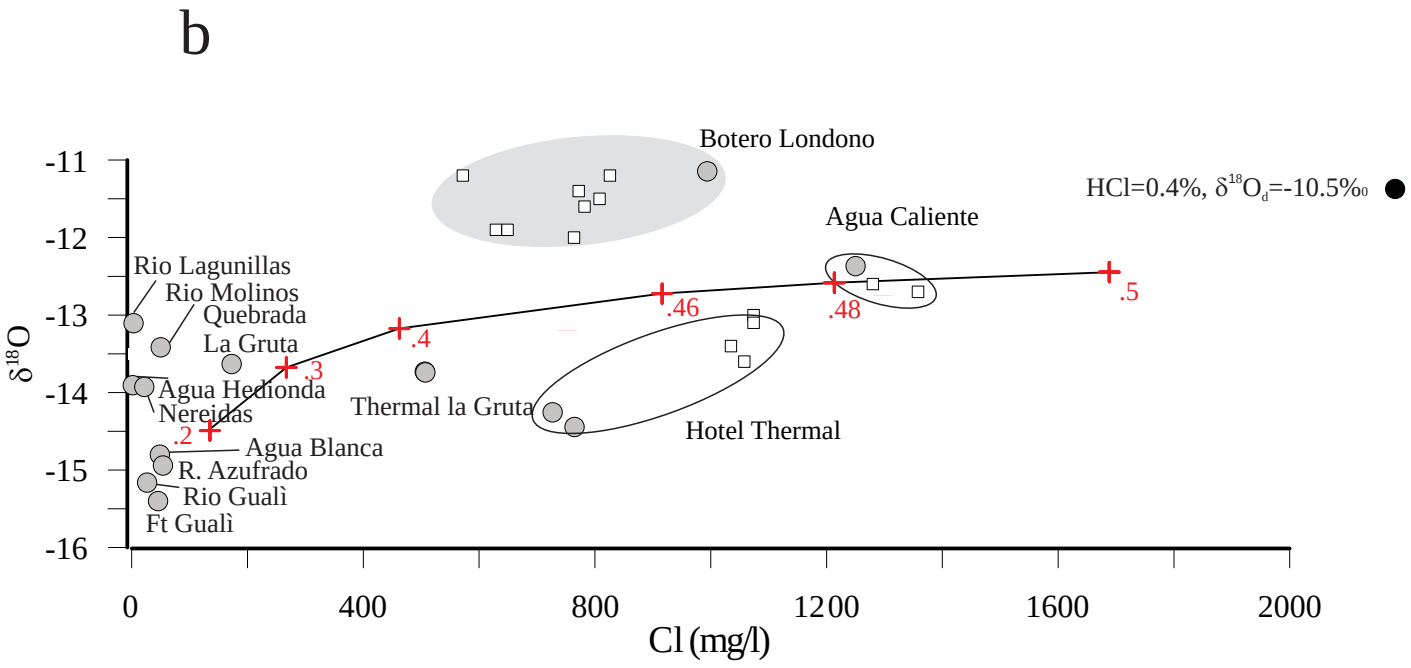

Figure 10

Figure 11

Click here to download Figure: Figure 11.pdf

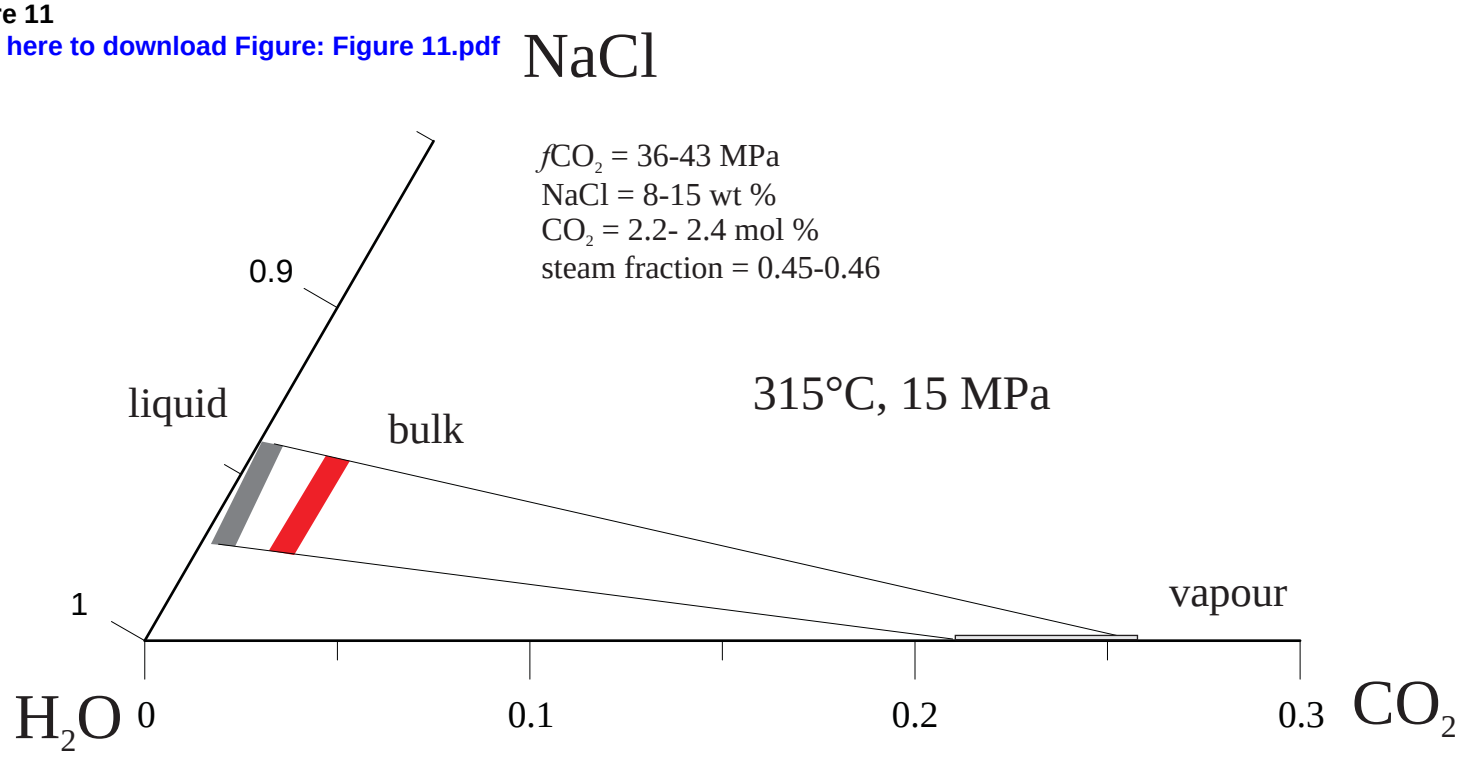

Figure 11